

Statistical mechanics of randomly polymerized membranes

Leo Radzihovsky and David R. Nelson

Department of Physics, Harvard University, Cambridge, Massachusetts 02138

(Received 5 April 1991)

The effect of quenched random internal disorder on tethered membranes is studied by modifying treatments of pure systems to allow for small local fluctuations in the metric due to defects. To lowest order in $\epsilon=4-D$, where D is the internal membrane dimensionality, we find that the flat pure phase is stable to disorder at finite temperatures, but unstable at low temperatures to a phase that lies outside the range of the ϵ expansion. For $D < 4$ the instability is triggered by any finite amount of disorder, while for $D > 4$ there is a threshold value of disorder below which the flat phase is stable at all temperatures. We speculate on the nature of the new phase. We argue that the low-temperature instability persists in the presence of random spontaneous curvature, and show that the flat phase is *always* unstable when unbound disclinations are included in the disorder.

I. INTRODUCTION

“Tethered surfaces,” which are two-dimensional generalizations of linear polymer chains [1,2], have been the focus of a number of theoretical investigations during the past five years. Unlike conventional polymers, these objects are expected to exhibit a low-temperature flat phase [3], with long-range order in the normals and very large fluctuations perpendicular to the average membrane plane. Thus far, a high-temperature crumpled phase has only been seen in computer simulations of “phantom” membranes, with interactions between nearest-neighbor monomers only [4]. Recent computer simulations [5] suggest that simple triangulated membranes with further-neighbor self-avoidance are always flat, due to a large entropically induced bending rigidity [6]. Powerful theoretical techniques have been developed to treat the flat phase, where explicit distant-neighbor self-avoidance (provided one introduces a bending rigidity) is believed to be unimportant. Fluctuations can be treated by considering D -dimensional polymerized manifolds embedded in d dimensions, and then carrying out expansions in $\epsilon=4-D$ [7–9] or $1/d$ [9] to treat the physically relevant case $D=2$ and $d=3$.

Although precise laboratory experiments are just beginning, there are in fact many experimental realizations of polymerized membranes. Poly-methyl-methacrylate tethered surfaces were synthesized on the surface of sodium montmorillonite clay and then floated off over 20 years ago by A. Blumstein, R. Blumstein, and Vander-spurt [10]. The inner surface of red blood cells contains the fishnetlike biopolymer spectrin which can be extracted and studied in isolation from the lipid bilayer [11]. Red blood cells themselves, with the spectrin attached to the lipid cell wall, can also be described by these theories, as emphasized recently by Lipowsky and Girardet [12]. Leibler [13] has suggested that simple “paracrystals” of proteins like tropomyosin [14] provide another example of a biological tethered surface. Inorganic examples of tethered surfaces include graphite oxide sheets in an ap-

propriate solvent [15] and the “rag” sheetlike structures found in MoS_2 [16]. For other experimental realizations see Ref. [2].

Most investigations of sheet polymers to date have assumed a regular lattice of identical monomers bonded permanently to their nearest neighbors. Various kinds of inhomogeneous disorder, however, are an almost inevitable feature of the experimental systems discussed above. Examples of disorder include holes or tears in the polymerized network, variations in the local coordination number, and impurities incorporated at random into the polymerized net. *A priori*, one might not have expected a small amount of disorder to affect the “universal” long-wavelength properties of polymerized membranes [17]. It is known, for example, that random copolymerization with only repulsive interactions does not affect the properties of crumpled linear polymer chains in a good solvent [18]. As discussed below, similar arguments can be applied to the crumpled phase of membranes, assuming this exists. The elastic description of the *flat* phase of membranes requires only a well-defined bending rigidity and elastic constants. Using the methods of Refs. [8] and [9], it is easy to show that small quenched random spatial variations in the microscopic elastic constants and bending rigidity of the flat phase will not affect the results for pure systems. These conclusions are consistent with recent molecular-dynamics simulations by Grest and Murat on site-diluted tethered membranes, in which a flat phase persists right up to the percolation threshold [19].

The above kinds of disorder, however, *also* produce random inhomogeneities in the internal metric. A dilute concentration of large copolymerized monomers, for example, will warp the surface and alter the way distances are measured internally within the membrane. It was recently shown that quenched random variations in the local metric can destabilize the flat phase at sufficiently low temperatures [20]. In this paper we explore these ideas in detail. We consider general quenched random perturbations about a locally flat metric, as might arise in a model with both inhomogeneous particles sizes and bond

lengths (see Fig. 1). D -dimensional tethered manifolds embedded in d dimensions [7–9] are studied to lowest order in an expansion in $\epsilon=4-D$. Below $D=4$, disorder softens the bending rigidity and destabilizes the flat phase at zero temperature. The flat phase can persist over a range of temperatures in the presence of weak disorder, but our results suggest a transition to disorder-dominated behavior at sufficiently low temperatures. For $D > 4$, a transition to a “glassy” phase dominated by disorder only occurs above a certain threshold disorder strength. Although the properties of the disorder-dominated regimes cannot be treated within the ϵ expansion, the possibility of a crumpled surface with Edwards-Anderson spin-glass order in the surface tangents can be explored in the limit

$d \rightarrow \infty$ [21].

Similar conclusions probably apply to surfaces with random holes and tears. Holes can be carefully excised at random from a triangular lattice with perfect sixfold coordination in such a way that the ground state is flat at zero temperature. At finite temperatures, however, the edges of these holes will contract (due to entropic effects) more than the unexcised regions, leading again to strains associated with perturbations in the local metric. These arguments suggest a possible instability of the flat phase in this limit of low but finite temperatures and large elastic constants in simulations like those of Grest and Murat [19].

The results described above apply to surfaces that retain a simple sixfold triangular bonding topology. Compact membranes can also be polymerized with identical monomers, but with defects in the sixfold bonding topology. The elementary defects in this case are points of fivefold and sevenfold coordination, i.e., disclinations. Suppose for simplicity that the polymerization is carried out in an essentially flat environment, e.g., in a Langmuir-Blodgett film at an air-water interface. We can then study the conformations of such a membrane when placed in an approximately neutral solvent, such as alcohol [22]. The defects that result from polymerizing a finite-temperature solid will be primarily bound pairs of dislocations, each of which can be regarded as a 5-7 disclination dipole [23]. We shall argue in Sec. III that the behavior in this case resembles the random-impurity problem discussed above. Membranes formed by polymerizing a liquid, on the other hand, will have unbound disclinations embedded in the bonding topology. We show that this leads to long-range correlations in the random metric and *always* destabilizes the flat phase of pure systems, even at finite temperatures. We find, however, that unbound *dislocations*, which would appear in an intermediate hexatic phase [23], are by themselves insufficient to destabilize the flat phase at finite temperatures.

An important recent experiment by Mutz, Bensimon, and Brienne [24] has led us to consider one additional kind of randomness. These authors study polymerized vesicles, i.e., closed surfaces made of lipid bilayers. In the absence of polymerization, these materials exhibit a remarkable shape transformation from a spherical topology to a cylindrical one with decreasing temperature. The transformation appears to be associated with the expulsion of Gaussian curvature as hexatic or crystalline order develops within the membrane [25]. If the vesicles at high temperature are first subjected to polymerizing ultraviolet radiation, a remarkable “wrinkling transition” to a rigid glassy phase takes place at about the temperature where the shape transformation occurs in unpolymers samples. The partial polymerization at high temperatures presumably results in sparse but percolating networks of covalent bonds that prevent the shape transformation. As this material cools, crystalline order sets in within these lipid “corrals,” and quenched random strains, similar to those discussed above, will develop. There are, however, two additional complications: (1) If the initial polymerization is in a *liquid*, as opposed to a

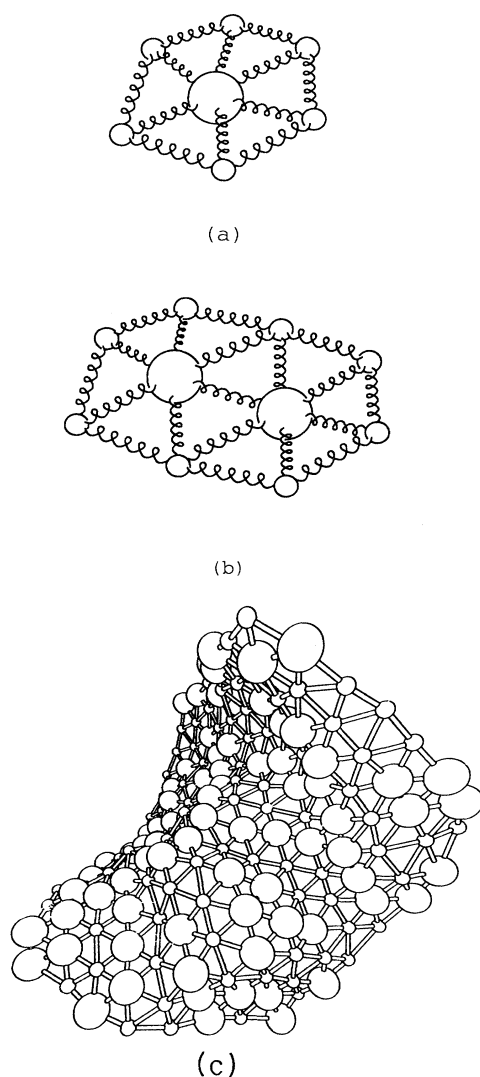


FIG. 1. Examples of impurity disorder. (a) Isolated large impurity in a matrix of smaller monomers. (b) Two impurities in close proximity forming an exceptionally long bond, embedded in a matrix of small monomers. (c) Relaxed configuration of many large impurities in a tethered membrane (courtesy of Y. Kantor).

hexatic phase, unbound disclinations will be an important component of the disorder. The observed wrinkling presumably reflects the disclination-induced instability of the flat phase discussed above [26]. (2) Because of spatial variations in the amount of polymerization on different sides of the bilayer, quenched random fluctuations in the *spontaneous* curvature will also appear.

To treat the complication (2) above, we show here that small fluctuations in the spontaneous curvature about zero [27] do not affect our conclusions about the instability of the flat phase at low temperatures in the presence of random strains and disclinations for the case $D=2$ and $d=3$. The transition observed by Mutz, Bensiman, and Brienne is thus an excellent candidate for the instability predicted in this paper. It would also be interesting to study the effects of a random spontaneous curvature within the ϵ expansion [28].

We conclude by emphasizing some limitations of our analysis. Although we show that the flat phase is unstable under certain conditions, we can only speculate about the asymptotic long-distance behavior in this case. Our results strongly suggest some sort of glassy behavior for $d=3$ and $D=2$ (see Sec. V), and a crumpled membrane spin glass may well result in the limit $d \rightarrow \infty$ [21]. Even these calculations, however, suffer from the neglect of distant self-avoidance. Distant-neighbor self-avoidance, although unimportant in the flat phase, may well affect the physics of any “spin-glass” phases. One possibility is a “roughened” glass phase that is macroscopically flat, but with a different roughness exponent than for pure systems.

In Sec. II we define our model and argue that random impurities do not affect the crumpled phase of phantom and self-avoiding membranes. A straightforward application of the Harris criterion [29], however, shows that such randomness is important at the crumpling transition itself for phantom membranes. When unbound disclinations are present, we find a logarithmically divergent swelling in the crumpled phase of phantom membranes. In Sec. III we discuss the flat phase via perturbation theory for $D=2$ and $d=3$, focusing on the renormalized bending rigidity. We find that (i) random impurity disorder destabilizes the flat phase at zero temperature while leaving it intact at finite temperatures; (ii) a quenched distribution of unbound disclinations embedded in a membrane destabilizes the flat-phase characteristic of pure systems at *all* temperatures; and finally (iii) random spontaneous curvature does not affect results (i) and (ii). The ϵ -expansion results for general Gaussian quenched random fluctuations about a flat metric caused by random impurities are described in Sec. IV, confirming the conclusions (i) above. Section V contains some conclusions and arguments for spin-glass order in membranes at low temperatures. The details of the ϵ expansion, as well as the rederivation of our results using the replica trick, are contained in three appendices.

II. MODEL FREE ENERGY WITH DISORDER

A. Pure systems

We define the polymerized membrane with a lattice model of a flexible D -dimensional sheet of interconnected

particles fluctuating in the embedding d -dimensional space. We use periodic boundary conditions to mimic an open topology. The connectivity of the tethered membrane allows us to label the constituent particles with a D -dimensional vector \mathbf{x} . We specify the embedding of these particles inside the d -dimensional space with a continuous d -dimensional vector $\vec{r}(\mathbf{x})$. Because here we are only interested in the large-distance physics, with the usual coarse graining, we pass to a continuum field theoretic model. This transformation allows us to describe the membrane by a D -dimensional manifold with a coordinate system $\{x_\alpha\}$ attached to it, embedded inside a d -dimensional Euclidean space. This naturally induces a metric for the hypersurface as a pull back from the embedding space

$$g_{\alpha\beta} = \partial_\alpha \vec{r} \cdot \partial_\beta \vec{r}. \quad (2.1)$$

For membranes without impurities with a flat ground state at $T=0$, we can always select coordinates x_α such that the configuration

$$\vec{r}^0 = \zeta [x_1, x_2, \dots, x_D, 0, 0, \dots, 0] \quad (2.2)$$

minimizes the free energy. The corresponding ground-state metric is

$$g_{\alpha\beta}^0 = \partial_\alpha \vec{r}^0 \cdot \partial_\beta \vec{r}^0 = \zeta^2 \delta_{\alpha\beta}. \quad (2.3)$$

We require that the continuum field theoretic model respects all the original symmetries of the underlying lattice model, and construct an effective free energy that is invariant under translations and rotations in the d -dimensional space and is $O(D)$ invariant. Translational invariance requires that the Landau-Ginzburg effective Hamiltonian must be an expansion in powers of the tangent vectors $\vec{t}_\alpha = \partial_\alpha \vec{r}(\mathbf{x})$ [7],

$$\mathcal{F}_{\text{eff}}[\vec{r}] = \int d^D \mathbf{x} \left[\frac{1}{2} \kappa (\partial_\alpha^2 \vec{r})^2 + \frac{1}{2} t (\partial_\alpha \vec{r})^2 + u (\partial_\alpha \vec{r} \cdot \partial_\beta \vec{r})^2 + \bar{v} (\partial_\alpha \vec{r} \cdot \partial_\alpha \vec{r})^2 \right]. \quad (2.4)$$

In the above expansion we exclude distant-neighbor interactions, restricting our attention to phantom membranes or the flat phase of self-avoiding ones. Upon identifying the tangents $[\vec{t}_\alpha = \partial_\alpha \vec{r}(\mathbf{x})]$ as the order parameters of this field theory, an analogy with the usual ϕ^4 theories of critical phenomena becomes apparent [7].

Within mean-field theory the high-temperature crumpled phase of the membrane is characterized by a positive value of coupling constant t . At low temperatures, however, the microscopic surface tangents, or equivalently the normals, tend to align, thereby minimizing the bending energy and forming a flat phase described by a negative t . It can be shown that the minimum of Eq. (2.4) is then given by Eq. (2.2) with [7]

$$\zeta = \frac{1}{2} \left[\frac{-t}{u + D\bar{v}} \right]^{1/2}. \quad (2.5)$$

The nonlinear quartic terms are now essential to stabilize the membrane.

B. Inclusion of disorder

We now extend the model for the pure membrane to include the effects of the quenched random impurity disorder. We first assume $t < 0$, and then rewrite the effective free energy for the pure membrane in the suggestive form [7,9]

$$\mathcal{F}_{\text{eff}}[\bar{\mathbf{r}}] = \int d^D x \left[\frac{1}{2} \kappa (\partial_\alpha \bar{\mathbf{r}})^2 + \mu (u_{\alpha\beta})^2 + \frac{1}{2} \lambda (u_{\alpha\alpha})^2 \right], \quad (2.6)$$

where μ and λ are Lamé coefficients, related to the previous coupling constants by $\mu = 4u\zeta^4$ and $\lambda = 8\bar{v}\zeta^4$. The quantity $u_{\alpha\beta}$ is the strain tensor, defined by

$$u_{\alpha\beta} = \frac{1}{2\zeta^2} (g_{\alpha\beta} - g_{\alpha\beta}^0) \quad (2.7a)$$

$$= \frac{1}{2\zeta^2} (\partial_\alpha \bar{\mathbf{r}} \cdot \partial_\beta \bar{\mathbf{r}} - \partial_\alpha \bar{\mathbf{r}}^0 \cdot \partial_\beta \bar{\mathbf{r}}^0). \quad (2.7b)$$

The strain tensor measures the local deformation of the membrane relative to the metric in the ground state. For the pure system this reference metric $g_{\alpha\beta}^0$ is always taken to be flat, as in Eq. (2.3). However, in the presence of disorder, the reference metric $g_{\alpha\beta}^0$ will be modified to reflect local deformations of the membrane to accommodate defects and impurities. These deformations will be small if the size of the impurity molecules is not too different from the size of the host molecules. This leads us to model the effects of the random impurities by taking $g_{\alpha\beta}^0$ to be

$$g_{\alpha\beta}^0 = \partial_\alpha \bar{\mathbf{r}}^0 \cdot \partial_\beta \bar{\mathbf{r}}^0 = \zeta^2 [\delta_{\alpha\beta} + 2c_{\alpha\beta}(\mathbf{x})], \quad (2.8)$$

where $c_{\alpha\beta}(\mathbf{x})$ is a new quenched random field with a probability distribution

$$\mathcal{P}[c_{\alpha\beta}(\mathbf{x})] \propto \exp \left[-\frac{1}{2\sigma_1 D^2} \int d^D x (c_{\alpha\alpha})^2 - \frac{1}{2\sigma_2} \int d^D x (\hat{c}_{\alpha\beta})^2 \right] \quad (2.9)$$

for spatially uncorrelated impurities. In Eq. (2.9) we have separated the quenched field $c_{\alpha\beta}$ into the traceless part $\hat{c}_{\alpha\beta} = c_{\alpha\beta} - (1/D)\delta_{\alpha\beta} c_{\gamma\gamma}$ and the trace $c_{\alpha\alpha}$. The parameters σ_1 and σ_2 can be viewed as frozen-in ‘‘temperatures’’ characterizing the isotropic and anisotropic parts of quenched defect distribution. When $\sigma_2 \rightarrow 0$, we recover the case of isotropic impurity disorder $c_{\alpha\beta}(\mathbf{x}) = c(\mathbf{x})\delta_{\alpha\beta}$ discussed in Refs. [20,30]. As is usual in problems with quenched disorder, we assume that it is the free energy rather than the partition function that should be averaged over this probability distribution.

In Secs. III and IV we shall study the response of this system to both disorder and thermal fluctuations by expanding about the flat state, setting $\bar{\mathbf{r}}(\mathbf{x}) = (x_\alpha + u_\alpha)\bar{\mathbf{e}}_\alpha + f_\beta \bar{\mathbf{e}}_\beta$, where the $u_\alpha(\mathbf{x})$ are ‘‘in-plane’’ phonon coordinates, and the $f_\beta(\mathbf{x})$ multiply vectors $\{\bar{\mathbf{e}}_\beta, \beta = D+1, \dots, d\}$ which span a subspace perpendicular to the average manifold plane. In the special case $\kappa \rightarrow \infty$, extrinsic curvature is squeezed out, and we can set the $f_\beta = 0$. When $D=2$, the free energy Eq. (2.6) then

reduces to a model of flat crystalline films with a quenched random distribution of impurities [31]. In this case, the local dilations and contractions produced by the disorder lead to a reentrant dislocation unbinding transition into a disorder-dominated regime at sufficiently low temperatures. Of course, dislocations (and disclinations) in the *polymerized* net studied here, if they occur at all, are frozen in and cannot unbind. We defer a detailed discussion of this type of disorder to Sec. III C, and assume for now that the membrane retains the sixfold bonding topology of a triangular lattice.

C. Effect of disorder at high temperatures and at the crumpling transition

When $T > T_c$, i.e., for $t > 0$, the free energy Eq. (2.6) takes the form

$$\begin{aligned} \mathcal{F}_{\text{eff}}[\bar{\mathbf{r}}] = \int d^D x & \left[\frac{1}{2} \kappa (\partial_\alpha \bar{\mathbf{r}})^2 + \frac{1}{2} t (\partial_\alpha \bar{\mathbf{r}})^2 \right. \\ & + u (\partial_\alpha \bar{\mathbf{r}} \cdot \partial_\beta \bar{\mathbf{r}})^2 + \bar{v} (\partial_\alpha \bar{\mathbf{r}} \cdot \partial_\alpha \bar{\mathbf{r}})^2 \\ & + \gamma c_{\alpha\alpha}(\mathbf{x}) (\partial_\beta \bar{\mathbf{r}})^2 \\ & \left. + \gamma' c_{\alpha\beta}(\mathbf{x}) \partial_\alpha \bar{\mathbf{r}} \cdot \partial_\beta \bar{\mathbf{r}} \right], \quad (2.10) \end{aligned}$$

with

$$\gamma = \frac{t\bar{v}}{u + D\bar{v}}, \quad (2.11a)$$

$$\gamma' = \frac{tu}{u + D\bar{v}}, \quad (2.11b)$$

and where we have neglected terms that drop out of quenched averages. A useful measure of the size of the membrane in this high-temperature phase is the correlation function [1]

$$\begin{aligned} \overline{\langle |\bar{\mathbf{r}}(\mathbf{x}) - \bar{\mathbf{r}}(0)|^2 \rangle} \\ = 2 \frac{1}{(2\pi)^2} \int d^2 q \overline{\langle |\bar{\mathbf{r}}(\mathbf{q})|^2 \rangle} (1 - e^{i\mathbf{q}\cdot\mathbf{x}}), \quad (2.12) \end{aligned}$$

where the brackets represent a thermal average, the bar represents an average over the quenched random disorder, and $\bar{\mathbf{r}}(\mathbf{q})$ is the Fourier transform of $\bar{\mathbf{r}}(\mathbf{x})$.

For pure systems at high temperatures, the terms proportional to κ , u , and \bar{v} in Eq. (2.10) produce only small corrections to the basic result,

$$\langle |\bar{\mathbf{r}}(\mathbf{q})|^2 \rangle \approx \frac{1}{tq^2}, \quad (2.13)$$

and it follows that [1]

$$\lim_{x \rightarrow \infty} \langle |\bar{\mathbf{r}}(\mathbf{x}) - \bar{\mathbf{r}}(0)|^2 \rangle \approx \frac{1}{\pi t} \ln(x/a), \quad (2.14)$$

where a is a microscopic cutoff. A measure of the membrane size R_G in the high-temperature crumpled phase is this correlation function evaluated at $x \approx L$, where L is a typical membrane internal dimension [1]:

$$\begin{aligned} R_G &= [\langle |\bar{\mathbf{r}}(\mathbf{x}) - \bar{\mathbf{r}}(0)|^2 \rangle]_{x=L}^{1/2} \\ &\approx \frac{1}{(\pi t)^{1/2}} \ln^{1/2}(L/a). \quad (2.15) \end{aligned}$$

To see how disorder changes this result, we again neglect κ , u , and \bar{v} and expand in the couplings proportional to γ and γ' . The result for $\langle |\bar{r}(\mathbf{q})|^2 \rangle$ before and after averaging over disorder is depicted graphically in Fig. 2. This leads to a renormalization of t in Eq. (2.13),

$$t_R = t - \frac{2(2\gamma + \gamma')^2}{t} \frac{1}{(2\pi)^2} \int d^2k \sigma_1(\mathbf{k}) - \frac{2\gamma'^2}{t} \frac{1}{(2\pi)^2} \int d^2k \sigma_2(\mathbf{k}), \quad (2.16)$$

where $\sigma_1(\mathbf{k})$ and $\sigma_2(\mathbf{k})$ are wave-vector-dependent generalizations of the disorder strengths that appear in Eq. (2.9). Since we expect that $\sigma_1(\mathbf{k})$ and $\sigma_2(\mathbf{k})$ tend to constants at long wavelengths for uncorrelated impurity disorder, we see that there is only a finite downward renormalization of t , leading to a larger coefficient in Eq. (2.15). Thus weak impurity disorder merely swells the membrane slightly and should not affect the universal long-wavelength properties of phantom membranes in the crumpled phase.

We shall argue in Sec. III C that a quenched array of unbound disclinations in a membrane polymerized from an equilibrium two-dimensional liquid can be modeled by *correlated* disorder which satisfies $\sigma_2(\mathbf{k})=0$ and

$$\sigma_1(\mathbf{k}) \sim \frac{1}{|\mathbf{k}|^2}. \quad (2.17)$$

We see from Eq. (2.16) that there is then a logarithmically divergent renormalization of t in this case. We hope to study how disclinations increase the size of phantom membranes under these circumstances in a future publication.

Returning to impurity disorder without disclinations, we can show that these defects will in fact change the behavior of phantom membranes precisely at the crumpling transition. The term proportional to γ in Eq. (2.10), in particular, couples the disorder to the membrane “energy density” $(\partial_\alpha \bar{r})^2$. Taking over standard arguments due to Harris [29], we find that the pure system is only stable to disorder if the exponent of the specific heat is negative. Since the specific heat appears to *diverge* when $d=3$ and $D=2$ [4], disorder should lead to a new critical behavior

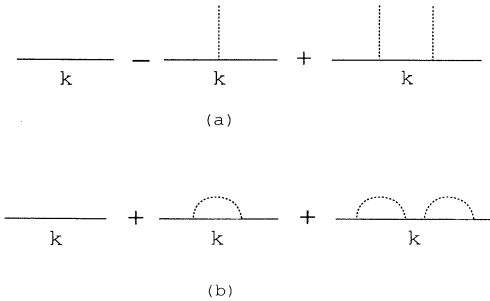


FIG. 2. Two-point correlation function in the high-temperature phase (a) before the quenched average, (b) after the quenched average.

at the crumpling transition in phantom membranes.

It is not yet clear if a crumpling transition exists for self-avoiding membranes [5]. The size R_G of a self-avoiding membrane in a high-temperature crumpled phase, if it exists, is expected to scale according to

$$R_G \sim L^\nu, \quad (2.18)$$

with [1] $\nu \approx \frac{4}{5}$. Random copolymerization will produce quenched fluctuations in the strength of the repulsive interactions between distant monomers, in addition to the terms discussed above. Obukhov [18] has shown using Flory arguments that these fluctuations have little effect on conventional linear polymers in a good solvent, i.e., above the Θ point. It is straightforward to adapt this approach and show that there are only small changes to Eq. (2.18) in the limit $L \rightarrow \infty$ for self-avoiding crumpled membranes as well.

III. PERTURBATION THEORY FOR $D=2$, $d=3$

Useful information about the physics of membranes can be obtained by simply expanding about the flat state. Using numerical and analytical information about the behavior of pure systems, we can study the stability of the flat phase to various kinds of disorder using this approach. We concentrate in this section on the case of experimental interest, $D=2$ and $d=3$.

A. Impurity disorder

Upon setting

$$\bar{r}(\mathbf{x}) = \zeta \{ [x_\alpha + u_\alpha(\mathbf{x})] \bar{e}_\alpha + f(\mathbf{x}) \bar{e}_3 \}, \quad (3.1)$$

with $\alpha=1,2$ and $\bar{e}_3 = \bar{e}_1 \times \bar{e}_2$, the free energy (2.6), to leading order in gradients of the $u_\alpha(\mathbf{x})$ and $f(\mathbf{x})$, reduces to

$$\mathcal{F}_{\text{eff}}[u_\alpha, f, c_{\alpha\beta}] = \int d^2x \left[\frac{1}{2} \kappa (\partial_\alpha^2 f)^2 + \mu (u_{\alpha\beta}^0)^2 + \frac{1}{2} \lambda (u_{\alpha\beta}^0)^2 - 2\mu c_{\alpha\beta} u_{\alpha\beta}^0 - \lambda c_{\beta\beta} u_{\alpha\alpha}^0 \right], \quad (3.2)$$

with

$$u_{\alpha\beta}^0(\mathbf{x}) = \frac{1}{2} (\partial_\alpha u_\beta + \partial_\beta u_\alpha + \partial_\alpha f \partial_\beta f). \quad (3.3)$$

We have neglected $O(c_{\alpha\beta}^2(\mathbf{x}))$ terms which drop out of quenched averages. The importance of disorder can be seen from a simple perturbative calculation of the renormalized bending rigidity κ_R . We first integrate out the in-plane phonon degrees of freedom, obtaining an effective free energy for the height function $f(\mathbf{x})$ as in the treatment of pure membranes [3],

$$e^{-\beta \mathcal{F}'_{\text{eff}}[f, c_{\alpha\beta}]} \equiv \int \mathcal{D}u_\alpha e^{-\beta \mathcal{F}_{\text{eff}}[u_\alpha, f, c_{\alpha\beta}]}, \quad (3.4)$$

where $\beta = 1/k_B T$ and

$$\mathcal{F}'_{\text{eff}} = \frac{1}{2} \kappa \int (\nabla^2 f)^2 d^2x + \frac{1}{2} K_0 \int \left[\frac{1}{2} P_{\alpha\beta}^T (\partial_\alpha f) (\partial_\beta f) - P_{\alpha\beta}^T c_{\alpha\beta}(\mathbf{x}) \right]^2 d^2x, \quad (3.5)$$

where $K_0 = 4\mu(\mu + \lambda)/(2\mu + \lambda)$ and $P_{\alpha\beta}^T$ is the transverse projection operator, $P_{\alpha\beta}^T = \delta_{\alpha\beta} - \partial_\alpha \partial_\beta / \nabla^2$.

We now calculate the renormalized disorder and wave-vector-dependent bending rigidity $\kappa_R^D(\mathbf{q})$ and the elastic parameter $K_R(\mathbf{q})$ defined by

$$\overline{\langle |f(\mathbf{q})|^2 \rangle}_c \equiv \frac{k_B T}{\kappa_R^D(\mathbf{q}) |\mathbf{q}|^4}, \quad (3.6a)$$

$$\begin{aligned} & \overline{\langle f(\mathbf{q}_1) f(\mathbf{q} - \mathbf{q}_1) f(\mathbf{q}_2) f(\mathbf{q}_2 - \mathbf{q}) \rangle}_c \\ & \equiv k_B T K_R(\mathbf{q}) P_{\alpha\beta}^T(\mathbf{q}) P_{\gamma\delta}^T(\mathbf{q}) q_{1\alpha} q_{1\beta} q_{2\gamma} q_{2\delta}, \end{aligned} \quad (3.6b)$$

where the bar represents an average over the quenched random impurity field and where c signifies that only the connected part of the correlation function is included. We have also divided out the momentum-conserving δ function in our definition of the averages. To leading order in $k_B T$ and the disorder strengths σ_1 and σ_2 , we obtain for the renormalized bending rigidity

$$\begin{aligned} \kappa_R^D(q) = & \kappa + k_B T \frac{1}{(2\pi)^2} \int d^2 p \frac{K_0 [\hat{q}_\alpha P_{\alpha\beta}^T(\mathbf{p}) \hat{q}_\beta]^2}{\kappa |\mathbf{q} + \mathbf{p}|^4} \\ & - (\sigma_1 + \sigma_2) \frac{1}{(2\pi)^2} \int d^2 p \frac{K_0^2 [\hat{q}_\alpha P_{\alpha\beta}^T(\mathbf{p}) \hat{q}_\alpha]^2}{\kappa |\mathbf{q} + \mathbf{p}|^4}, \end{aligned} \quad (3.7)$$

where there is an upper cutoff Λ implicit in the integrals corresponding to the underlying lattice model cell size. Although the above perturbation series is infrared divergent with the correction terms diverging like $1/q^2$, we can still extract the qualitative effects of thermal fluctuations and disorder on the ordered phase of the membrane. The first correction term is identical to the one for the pure tethered surface [3]. It shows that thermal fluctuations stiffen the membrane by increasing the bending rigidity. This term is responsible for the flat phase, since the diverging bending stiffness (obtained from a simple self-consistent theory [3]) tends to suppress the undulation modes, which normally destroy the ordered phase in $D=2$. The second disorder-generated term in Eq. (3.7), on the other hand, leads to a divergent *reduction* of the bending rigidity. Since the first term carries the factor of T while the disorder term does not, the effect of disorder will dominate at low temperatures. This low-temperature disorder-activated instability is the main subject of this paper. In Sec. V we shall argue that this softening of the bending rigidity leads to many nearly degenerate minima in the free energy and the spin-glass ordering at $T=0$.

Weak disorder should *not* affect the asymptotic behavior of membranes in the flat phase at sufficiently high temperatures, despite its importance at $T=0$. To see this, assume the disorder is so weak that we can replace the elastic constants on the right-hand side of Eq. (3.7) by wave-vector-dependent quantities $\kappa_R(p)$ and $K_R(p)$ renormalized only by thermal fluctuations. These are expected to be singular as p tends to zero [3,8], with $\kappa_R(p) \sim p^{-\eta_\kappa}$ and $K_R(p) \sim p^{\eta_u}$. In the notation of Ref. [8], we have $\eta_u = \eta_\perp = \eta_\parallel$. We can then rewrite Eq. (3.7) in the form

$$\kappa_R^D(\mathbf{q}) = \kappa_R(\mathbf{q})$$

$$- (\sigma_1 + \sigma_2) \frac{1}{(2\pi)^2} \int d^2 p \frac{K_R^2(\mathbf{p}) [\hat{q}_\alpha P_{\alpha\beta}^T(\mathbf{p}) \hat{q}_\beta]^2}{\kappa_R(\mathbf{q} + \mathbf{p}) |\mathbf{q} + \mathbf{p}|^4}. \quad (3.8)$$

Upon using the scaling relation [8] $2\eta_\kappa + \eta_u = 2$ (a consequence of rotational invariance), we see that weak disorder will produce only a small singular correction to $\kappa_R^D(q)$, $\kappa_R^D(q) = \kappa_R(q) [1 - \text{const}(\sigma_1 + \sigma_2) q^{\eta_u}]$, provided $\eta_u > 0$. This exponent is positive in the perturbative calculations of Aronovitz and Lubensky [8]; existing numerical work is also consistent with a (possibly small) positive value. Thus weak disorder is irrelevant in the flat phase at sufficiently high temperatures, provided the in-plane elastic constants tend to zero at long wavelengths ($\eta_u > 0$). These soft elastic constants make it easier for the membrane to screen out the strains induced by impurities.

We can also study perturbatively the renormalized elastic parameter $K_R = 4\mu_R(\mu_R + \lambda_R)/(2\mu_R + \lambda_R)$:

$$\begin{aligned} K_R(\mathbf{q}) = & K_0 \\ & - \frac{k_B T}{2} P_{\alpha\beta}^T(\mathbf{q}) P_{\gamma\delta}^T(\mathbf{q}) \frac{1}{(2\pi)^2} \int d^2 p \frac{K_0^2 p_\alpha p_\beta p_\gamma p_\delta}{\kappa |\mathbf{p}|^4 \kappa |\mathbf{q} - \mathbf{p}|^4}. \end{aligned} \quad (3.9)$$

We observe that to one-loop order K_R is reduced by thermal fluctuations, but is unaffected directly by the disorder.

B. Quenched random dislocations and disclinations

Virtually all calculations of polymerized membranes to date have excluded defects in the bonding topology, such as dislocations and disclinations [32]. We show here that a quenched array of such defects, embedded in a polymerized net that prefers equal bond lengths, can be modeled by a free energy like Eq. (3.5), provided we modify the distribution function of the randomness in Eq. (2.9).

Our starting point is the analysis of crystalline and fluid order on a random topography in Ref. [33]. This paper studies the effect of *annealed* dislocations and disclinations in membranes subjected to a *quenched* random out-of-plane displacement field $f(\mathbf{x})$. The starting point is just the effective free energy Eq. (3.2) with $c_{\alpha\beta}(\mathbf{x}) = 0$, with a frozen f field and a fixed distribution of disclinations and dislocations. If there are disclinations with ‘‘charges’’ $\{s_a\}$ at positions $\{\mathbf{x}_a\}$ and dislocations with Berger’s vectors $\{\mathbf{b}_b\}$ at positions $\{\mathbf{x}_b\}$, the total ‘‘disclination density’’ is [33]

$$s_{\text{tot}}(\mathbf{x}) = \sum_a s_a \delta(\mathbf{x} - \mathbf{x}_a) + \epsilon_{\alpha\beta} \sum_b b_{\alpha,b} \partial_\beta \delta(\mathbf{x} - \mathbf{x}_b). \quad (3.10)$$

Reference [33] then integrates out the in-plane phonon fields u_α . It is easy to carry out identical manipulations (i.e., those that lead to Eq. (3.17) of Ref. [33]) with a *quenched* distribution of dislocations and disclinations

and an *annealed* out-of-plane displacement field. The result is an effective free energy

$$\mathcal{F}'_{\text{eff}} = \frac{1}{2}\kappa \int (\nabla^2 f)^2 d^2x + \frac{1}{2}K_0 \int \left[\frac{1}{2}P_{\alpha\beta}^T (\partial_{\alpha} f)(\partial_{\beta} f) - c(\mathbf{x}) \right]^2 d^2x. \quad (3.11)$$

This has the same form as Eq. (3.5), with $c_{\alpha\beta} = c(\mathbf{x})\delta_{\alpha\beta}$. We find that $c(\mathbf{x})$ is related to the total disclination density via

$$\nabla^2 c(\mathbf{x}) = s_{\text{tot}}(\mathbf{x}). \quad (3.12)$$

We can now evaluate the renormalization of the bending rigidity exactly as in the previous subsection, provided we can extract the appropriate distribution for $c(\mathbf{x})$ using Eq. (3.12). The precise probability distribution depends on the circumstances of the polymerization. We focus for simplicity on polymerizations carried out at a finite temperature on an essentially flat membrane (e.g., a

Langmuir-Blodgett film at an air-water interface, or a liposome with a large bending rigidity), which is then allowed to fluctuate freely in a three-dimensional solvent. There are three cases to consider.

(i) If the polymerization is carried out on a finite-temperature crystal, disclinations exist only in tightly bound dipole pairs forming dislocations which are themselves bound together to form neutral disclination quadrupoles and sextets [23,34]. Tightly bound dislocation pairs are in fact equivalent to localized vacancy and interstitial defects in the solid [35]. The associated strains are very similar to those produced by impurities, so we expect a distribution function similar to Eq. (2.9).

(ii) If the polymerization is carried out at temperature T^* in a hexatic phase, unbound dislocations will be present. The probability distribution for the Fourier-transformed Burger's-vector field at long wavelengths is known to be [23]

$$\mathcal{P}_c[b_{\alpha}(\mathbf{q})] \propto \exp \left\{ -\frac{1}{2k_B T^*} \frac{1}{(2\pi)^2} \int d^2q \left[\frac{K^*}{q^2} \left[\delta_{\alpha\beta} - \frac{q_{\alpha}q_{\beta}}{q^2} \right] + E_c^* \delta_{\alpha\beta} \right] b_{\alpha}(\mathbf{q})b_{\beta}(-\mathbf{q}) \right\}, \quad (3.13)$$

where $K^* = 4\mu^*(\mu^* + \lambda^*)/(2\mu^* + \lambda^*)$ is related to the elastic constants μ^* and λ^* of the underlying solid and E_c is a dislocation core energy. All quantities with the superscript * refer to their values at the time and temperature of polymerization. Disclinations are presumably less important at long wavelengths in the hexatic phase because they remain bound in charge-neutral pairs. Upon neglecting the disclination term in Eq. (3.10), we combine Eqs. (3.10) and (3.12) to find $c(\mathbf{q}) = i\epsilon_{\alpha\beta}q_{\alpha}b_{\beta}(\mathbf{q})/q^2$, or

$$|c(\mathbf{q})|^2 = \frac{1}{q^2} \left[\delta_{\alpha\beta} - \frac{q_{\alpha}q_{\beta}}{q^2} \right] b_{\alpha}(\mathbf{q})b_{\beta}(\mathbf{q}), \quad (3.14)$$

which, in view of Eq. (3.13), leads to a probability distribution for $c(\mathbf{x})$ that has the long-wavelength form

$$\mathcal{P}_h[c(\mathbf{x})] \propto \exp \left[-\frac{K^*}{2k_B T^*} \int d^2x c^2(\mathbf{x}) \right]. \quad (3.15)$$

Polymerized hexatics can thus be described by Eq. (2.9) with $\sigma_2 = 0$ and

$$\sigma_1 = \frac{k_B T^*}{K^*}. \quad (3.16)$$

(iii) If the membrane is a polymerized liquid permeated by a gas of unbound disclinations, there are important new consequences. Screening by free dislocations leads to a relatively weak interactions between disclinations in the hexatic phase, an interaction which ultimately allows them to unbind above the hexatic-to-liquid transition temperature [23]. The probability distribution for the Fourier-transformed disclination density $s(\mathbf{q})$ is then

$$\mathcal{P}_s[s(\mathbf{q})] \propto \exp \left[\frac{-1}{2k_B T^*} \frac{1}{(2\pi)^2} \int d^2q \left[\frac{K_A^*}{q^2} + E_c^* \right] \times |s(\mathbf{q})|^2 \right], \quad (3.17)$$

where E_c is a disclination core energy and K_A^* is a hexatic stiffness constant related to a *dislocation* core energy [23]. Upon neglecting the Burger's-vector term in Eq. (3.10) [the effects of free dislocations are already incorporated into Eq. (3.17)], we find that Eq. (3.17) leads to a long-wavelength probability distribution for polymerized liquids of the form

$$\mathcal{P}_s[c(\mathbf{x})] \propto \exp \left[-\frac{K_A^*}{2k_B T^*} \int d^2x |\vec{\nabla} c(\mathbf{x})|^2 \right]. \quad (3.18)$$

This has the form of Eq. (2.9) provided we set $\sigma_2 = 0$ and allow for nontrivial wave-vector dependence in the Fourier-transformed variance

$$\sigma_1 \rightarrow \sigma_1(\mathbf{q}) = \frac{k_B T^*}{K_A^* q^2}. \quad (3.19)$$

Evidently, solids and hexatics polymerized at finite temperatures will behave much like defect-free membranes with impurity disorder. Polymerized liquids, on the other hand, are described by *correlated* randomness. This has important consequences. Upon repeating the analysis that led to Eq. (3.8), for example, we find that

$$\kappa_R^D(\mathbf{q}) = \kappa_R(\mathbf{q}) - \frac{k_B T^*}{K_A^*} \frac{1}{(2\pi)^2} \times \int d^2p \frac{K_R^2(\mathbf{p}) [\hat{q}_{\alpha} P_{\alpha\beta}^T(\mathbf{p}) \hat{q}_{\beta}]^2}{\kappa_R(\mathbf{q} + \mathbf{p}) |\mathbf{p}|^2 |\mathbf{q} + \mathbf{p}|^4}. \quad (3.20)$$

Because of the extra factor of $1/|\mathbf{p}|^2$, the integral is now much more singular, and we find that randomness is only negligible at the flat-phase fixed point, provided $\eta_u > 2$. This inequality is incompatible, however, with a diverging bending rigidity, in view of the relation $2\eta_{\kappa} + \eta_u = 2$. We conclude that the flat phase of polymerized liquids is

destabilized by unbound disclination disorder at all temperatures. A $6-\epsilon$ expansion would be necessary to control the quenched-random-strain fluctuations in this case.

C. Random spontaneous curvature

As discussed in the Introduction, recent experiments by Mutz *et al.* suggest that randomness in the locally preferred spontaneous curvature (as well as random strains) may be important in partially polymerized lipid bilayers [24]. We consider here the effect of a zero-mean quenched random spontaneous curvature variable $h(\mathbf{x})$. We assume that $h(\mathbf{x})$ is uncorrelated in space and characterized by a Gaussian distribution with variance Δ . We now consider a modification of Eq. (3.5), namely

$$\begin{aligned} \mathcal{F}[f, u_\alpha] = & \int d^2x \left\{ \frac{1}{2} \kappa [\nabla^2 f] - h \right\}^2 \\ & + \frac{1}{2} K_0 \left[\frac{1}{2} P_{\alpha\beta}^T (\partial_\alpha f) (\partial_\beta f) \right. \\ & \left. - P_{\alpha\beta}^T c_{\alpha\beta}(\mathbf{x}) \right]^2 \}. \end{aligned} \quad (3.21)$$

The extra term is similar to a random field acting on a spin system [36] except that it couples to the Laplacian of the fluctuating field $f(\mathbf{x})$. As in the random-field problem, the main effect of $h(\mathbf{x})$ (at least in the renormalization of the rigidity) is a modification of the f propagator,

$$\frac{k_B T}{\kappa |\mathbf{q}|^4} \rightarrow \frac{k_B T}{\kappa |\mathbf{q}|^4} + \frac{1}{\kappa |\mathbf{q}|^4} \Delta \kappa^2 |\mathbf{q}|^4 \frac{1}{\kappa |\mathbf{q}|^4}. \quad (3.22)$$

We again compute κ_R^D within this generalized model and find

$$\begin{aligned} \kappa_R^D(\mathbf{q}) = & \kappa + k_B T \frac{1}{(2\pi)^2} \int d^2p \frac{K_0 [\hat{q}_\alpha P_{\alpha\beta}^T(\mathbf{p}) \hat{q}_\beta]^2}{\kappa_{\text{eff}} |\mathbf{q} + \mathbf{p}|^4} \\ & - (\sigma_1 + \sigma_2) \frac{1}{(2\pi)^2} \int d^2p \frac{K_0^2 [\hat{q}_\alpha P_{\alpha\beta}^T(\mathbf{p}) \hat{q}_\beta]^2}{\kappa_{\text{eff}} |\mathbf{q} + \mathbf{p}|^4}, \end{aligned} \quad (3.23)$$

where $\kappa_{\text{eff}} = \kappa / (1 + \Delta \kappa / k_B T)$. We observe that the effect of extrinsic curvature disorder is simply to reduce κ , particularly at low temperatures. Identical conclusions apply when the expansion (3.20) appropriate to unbound disclinations is modified to allow for random spontaneous curvature.

We conclude that the low-temperature instabilities associated with random strains continue in the presence of randomness in the spontaneous curvature. The effect of random spontaneous curvature has recently been studied with the ϵ expansion by Morse and Lubensky [28].

IV. RENORMALIZATION GROUP AND THE EPSILON EXPANSION

To study the generalized model of D -dimensional manifolds embedded in d dimensions, we first set $\vec{r}(\mathbf{x}) = (x_\alpha + u_\alpha) \vec{e}_\alpha + f_\beta \vec{e}_\beta$ in Eq. (2.6), where the $\{u_\alpha(\mathbf{x})\}$ represent D in-plane phonon coordinates, and the $\{f_\beta(\mathbf{x})\}$ represent $d_c = d - D$ out-of-plane modes. Our goal is to study the scaling exponents η_κ , η_\perp , and η_\parallel by

looking at the long-distance scaling properties of the Fourier transformed \vec{r} and u_α two-point correlation functions [8], which are related to the renormalized coupling constants κ_R , μ_R , and λ_R ,

$$\overline{|\vec{r}(\mathbf{q})|^2} \equiv \frac{k_B T}{\kappa_R(q) q^4} \sim q^{-4+\eta_\kappa}, \quad (4.1a)$$

$$\overline{\langle |u_\alpha^T(\mathbf{q}) u_\beta^T(-\mathbf{q}) \rangle_c} \equiv P_{\alpha\beta}^T \frac{k_B T}{\mu_R(q) q^2} \sim q^{-2-\eta_\perp}, \quad (4.1b)$$

$$\overline{\langle |u_\alpha^L(\mathbf{q}) u_\beta^L(-\mathbf{q})|^2 \rangle_c} \equiv P_{\alpha\beta}^L \frac{k_B T}{[2\mu_R(q) + \lambda_R(q)] q^2} \sim q^{-2-\eta_\parallel}. \quad (4.1c)$$

In Eqs. (4.1) we have defined correlation functions of the transverse and longitudinal parts of the in-plane phonon degrees of freedom $u_\alpha^T \equiv P_{\alpha\beta}^T u_\beta$ and $u_\alpha^L \equiv P_{\alpha\beta}^L u_\beta$, respectively. The subscript c means that only connected parts are included. We wish to study the scaling exponents η_κ , η_\perp , and η_\parallel to first order in ϵ expansion as was done by other authors for pure membranes [8,9].

We first observe that in the mean-field-theory approximation the scaling exponents vanish, and κ_R , μ_R , and λ_R are wave-vector independent, consistent with the conventional elastic theory [37]. When the calculations of Sec. III are redone for D -dimensional manifolds, however, both the thermal and disorder-induced corrections to the bending rigidity diverge for all $D \leq 4$. Thus $D = 4$ is the upper-critical dimension of our theory.

We use the renormalization group to determine how the couplings in Eq. (2.6) scale for $D < 4$. The renormalization-group transformation described in Appendix A leads to the recursion relations

$$\kappa'(b) = \kappa, \quad (4.2a)$$

$$\mu'(b) = \mu b^{\epsilon - 2\eta_\kappa (1 - \eta_\perp \ln b)}, \quad (4.2b)$$

$$(2\mu + \lambda)'(b) = (2\mu + \lambda) b^{\epsilon - 2\eta_\kappa (1 - \eta_\parallel \ln b)}, \quad (4.2c)$$

$$\begin{aligned} \hat{\sigma}'_1(b) = & \hat{\sigma}_1 b^{\epsilon - 2\eta_\kappa} \left[1 - \left[\frac{2d_c A_D k_B T}{\kappa^2} \frac{D+1}{D^2+2D} \right. \right. \\ & \left. \left. \times \frac{\mu(2\mu+D\lambda)}{2\mu+\lambda} \right] \ln b \right], \end{aligned} \quad (4.2d)$$

$$\hat{\sigma}'_2(b) = \hat{\sigma}_2 b^{\epsilon - 2\eta_\kappa} \left[1 - \left[\frac{d_c A_D k_B T}{\kappa^2} \frac{4\mu}{D^2+2D} \right] \ln b \right], \quad (4.2e)$$

where $\hat{\sigma}_1 \equiv \sigma_1 A_D [2\mu(2\mu+D\lambda)/(2\mu+\lambda)]^2 / \kappa^2$, $\hat{\sigma}_2 \equiv \sigma_2 (2\mu)^2 / \kappa^2$, $d_c = d - D$, and $A_D = S_D / (2\pi)^D$, S_D being the surface area of a D -dimensional sphere. We have imposed a sharp cutoff and integrated out a fraction $1 - b^{-1}$ of the degrees of freedom, and have chosen rescalings of the \vec{r} and u_α fields that keep $\kappa'(b)$ fixed. The coefficients η_κ , η_\perp , and η_\parallel are given by

$$\eta_\kappa = \frac{D^2-1}{D^2+2D} \left\{ A_D k_B T \frac{4\mu(\mu+\lambda)}{\kappa^2(2\mu+\lambda)} - \hat{\sigma}_1 - \hat{\sigma}_2 \left[\frac{D-1}{D} \left[\frac{2\mu}{2\mu+\lambda} \right]^2 + \frac{2\lambda}{2\mu+\lambda} \right] \right\}, \quad (4.3a)$$

$$\eta_\perp = \frac{2d_c A_D k_B T}{D^2+2D} \frac{\mu}{\kappa^2}, \quad (4.3b)$$

$$\eta_\parallel = d_c A_D k_B T \frac{6\mu^2 + 2\mu\lambda(D+2) + \lambda^2(D^2+2D)/2}{(2\mu+\lambda)\kappa^2(D^2+2D)}. \quad (4.3c)$$

It is apparent from Eqs. (4.2a)–(4.2e) that the actual expansion is in powers of the effective coupling constants $\hat{\mu} \equiv A_D k_B T(\mu/\kappa^2)$ and $\hat{\lambda} \equiv A_D k_B T(\lambda/\kappa^2)$. The differential recursion relations for the running coupling constants $\hat{\mu}(l)$, $\hat{\lambda}(l)$, $\hat{\sigma}_1(l)$, and $\hat{\sigma}_2(l)$, with $b = e^l$, to lowest order in $\epsilon = 4 - D$, are then

$$\frac{d\hat{\mu}}{dl} = \epsilon\hat{\mu} - \frac{d_c}{12}\hat{\mu}^2 - \frac{5\hat{\mu}^2(\hat{\mu}+\hat{\lambda})}{2\hat{\mu}+\hat{\lambda}} + \frac{5}{4}\hat{\mu}\hat{\sigma}_1 + \frac{5}{4}\hat{\mu}\hat{\sigma}_2 \left[\frac{3\hat{\mu}^2}{(2\hat{\mu}+\hat{\lambda})^2} + \frac{2\hat{\lambda}}{2\hat{\mu}+\hat{\lambda}} \right], \quad (4.4a)$$

$$\frac{d\hat{\lambda}}{dl} = \epsilon\hat{\lambda} - \frac{d_c}{12}(\hat{\mu}^2 + 6\hat{\mu}\hat{\lambda} + 6\hat{\lambda}^2) - \frac{5\hat{\mu}\hat{\lambda}(\hat{\mu}+\hat{\lambda})}{2\hat{\mu}+\hat{\lambda}} + \frac{5}{4}\hat{\lambda}\hat{\sigma}_1 + \frac{5}{4}\hat{\lambda}\hat{\sigma}_2 \left[\frac{3\hat{\mu}^2}{(2\hat{\mu}+\hat{\lambda})^2} + \frac{2\hat{\lambda}}{2\hat{\mu}+\hat{\lambda}} \right], \quad (4.4b)$$

$$\frac{d\hat{\sigma}_1}{dl} = \epsilon\hat{\sigma}_1 - \frac{5d_c}{6} \frac{\hat{\sigma}_1\hat{\mu}(\hat{\mu}+2\hat{\lambda})}{2\hat{\mu}+\hat{\lambda}} - \frac{5\hat{\sigma}_1\hat{\mu}(\hat{\mu}+\hat{\lambda})}{2\hat{\mu}+\hat{\lambda}} + \frac{5}{4}\hat{\sigma}_1^2 + \frac{5}{4}\hat{\sigma}_1\hat{\sigma}_2 \left[\frac{3\hat{\mu}^2}{(2\hat{\mu}+\hat{\lambda})^2} + \frac{2\hat{\lambda}}{2\hat{\mu}+\hat{\lambda}} \right], \quad (4.4c)$$

$$\frac{d\hat{\sigma}_2}{dl} = \epsilon\hat{\sigma}_2 - \frac{d_c}{6} \hat{\sigma}_2\hat{\mu} - \frac{5\hat{\sigma}_2\hat{\mu}(\hat{\mu}+\hat{\lambda})}{2\hat{\mu}+\hat{\lambda}} + \frac{5}{4}\hat{\sigma}_1\hat{\sigma}_2 + \frac{5}{4}\hat{\sigma}_2^2 \left[\frac{3\hat{\mu}^2}{(2\hat{\mu}+\hat{\lambda})^2} + \frac{2\hat{\lambda}}{2\hat{\mu}+\hat{\lambda}} \right]. \quad (4.4d)$$

These β functions determine the flow of the coupling constants under the renormalization-group transformation.

They are rederived using the replica method in Appendix B. At $T=0$, these recursion relations simplify. The couplings $\hat{\mu}$ and $\hat{\lambda}$ remain fixed at zero, and

$$\frac{d\hat{\sigma}_1}{dl} = \epsilon\hat{\sigma}_1 + \frac{5}{4}\hat{\sigma}_1(\hat{\sigma}_1 + \hat{\sigma}_2 m), \quad (4.5a)$$

$$\frac{d\hat{\sigma}_2}{dl} = \epsilon\hat{\sigma}_2 + \frac{5}{4}\hat{\sigma}_2(\hat{\sigma}_1 + \hat{\sigma}_2 m), \quad (4.5b)$$

where

$$m = \lim_{T \rightarrow 0} \left[\frac{3\hat{\mu}^2}{(2\hat{\mu}+\hat{\lambda})^2} + \frac{2\hat{\lambda}}{2\hat{\mu}+\hat{\lambda}} \right]. \quad (4.6)$$

Note that the same combination of disorder variables $\hat{\sigma}_{\text{eff}} \equiv \hat{\sigma}_1 + m\hat{\sigma}_2$ enters both Eqs. (4.5a) and (4.5b). The recursion relations lead to four isolated fixed points for $\epsilon > 0$ and a line of fixed points at $T=0$ for $\epsilon < 0$ (see Table I).

The first four fixed points are identical to the ones obtained in the previous study of pure membranes [8]. They are confined to the $\hat{\sigma}_1 = \hat{\sigma}_2 = 0$ subspace, characterizing a membrane with no disorder. Below four dimensions the four fixed points characterizing the pure membrane are the only physical ones. P_1 is an infrared unstable Gaussian fixed point at the origin. P_2 and P_3 are partially unstable fixed points and lie on the boundary of the domain of stability of the membrane. The infrared stable fixed point P_4 characterizes the flat phase of a pure membrane. The scaling exponents η_κ , η_\perp and η_\parallel , evaluated at P_4 , lead to a diverging $\kappa_R(q)$ that stabilizes the flat phase and vanishing wave-vector-dependent elastic constants $\mu_R(q)$ and $\lambda_R(q)$. The eigenvalues for σ_1 and σ_2 at the fixed point P_4 are both $y_\sigma = -\epsilon/(1+24/d_c) = -\eta_\perp = -\eta_\parallel$, in agreement with the general perturbative argument for the stability of the flat phase presented in Sec. III A. At vanishing temperatures, however, the flow heads away toward the strong disorder region, which lies outside of the range of the ϵ expansion. This signifies that at low temperatures the flat phase of a pure membrane is unstable to a phase characterized by strong disorder that lies outside of the range of validity of the ϵ expansion (see Fig. 3).

The renormalization-group analysis leads to the scaling properties of the renormalized coupling constants

$$\kappa_R(q, \hat{\mu}, \hat{\lambda}, \hat{\sigma}_{\text{eff}}) = \exp \left[\int_0^l \eta_\kappa(l') dl' \right] \times \kappa_R(e^l q, \hat{\mu}(l), \hat{\lambda}(l), \hat{\sigma}_{\text{eff}}(l)), \quad (4.7a)$$

TABLE I. Fixed-point values of the coupling constants $\hat{\mu}$, $\hat{\lambda}$, and $\hat{\sigma}_{\text{eff}} = \hat{\sigma}_1 + m\hat{\sigma}_2$.

	$\epsilon > 0$				$\epsilon < 0$	
	P_1	P_2	P_3	P_4	P_1	P_5
$\hat{\mu}^*$	0	0	$\frac{12\epsilon}{20+d_c}$	$\frac{12\epsilon}{24+d_c}$	0	0
$\hat{\lambda}^*$	0	$2\epsilon/d_c$	$\frac{-6\epsilon}{20+d_c}$	$\frac{-4\epsilon}{24+d_c}$	0	0
$\hat{\sigma}_{\text{eff}}^*$	0	0	0	0	0	$-4\epsilon/5$

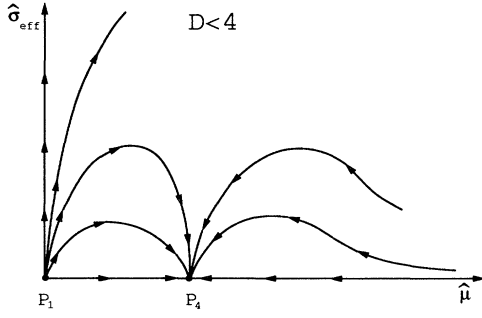


FIG. 3. Flow diagram for $D < 4$ showing instability at $T=0$.

$$\mu_R(q, \hat{\mu}, \hat{\lambda}, \hat{\sigma}_{\text{eff}}) = \exp \left[- \int_0^l \eta_{\perp}(l') dl' \right] \times \mu_R(e^l q, \hat{\mu}(l), \hat{\lambda}(l), \hat{\sigma}_{\text{eff}}(l)), \quad (4.7b)$$

$$(2\mu_R + \lambda_R)(q, \hat{\mu}, \hat{\lambda}, \hat{\sigma}_{\text{eff}}) = \exp \left[- \int_0^l \eta_{\parallel}(l') dl' \right] \times (2\mu_R + \lambda_R)(e^l q, \hat{\mu}(l), \hat{\lambda}(l), \hat{\sigma}_{\text{eff}}(l)). \quad (4.7c)$$

Upon choosing the rescaling parameter $l=l^*$ such that the rescaled momentum $q'(l^*)=e^{l^*}q=1$ we obtain the scaling forms defined in Eqs. (4.1). The scaling functions from Eqs. (4.3) evaluated at P_4 give the scaling exponents $\eta_{\kappa}=\epsilon/(2+d_c/12)$ and $\eta_{\perp}=\eta_{\parallel}=\epsilon/(1+24/d_c)$ characterizing the nontrivial flat phase of a pure membrane, in agreement with Ref. [8].

For $D > 4$ there is an unstable line of fixed points at $T=0$, i.e., for $\hat{\mu}=\hat{\lambda}=0$, given by

$$\hat{\sigma}_{\text{eff}}^* = \hat{\sigma}_1^* + m \hat{\sigma}_2^* = \frac{4}{3} |\epsilon|. \quad (4.8)$$

The zero-temperature renormalization-group flows associated with Eqs. (4.5) are shown in Fig. 4. We observe that if the initial amount of disorder is below the threshold line defined in Eq. (4.8) then the pure phase of the membrane, characterized by the Gaussian fixed point P_1 , is stable. However, for disorder larger than the critical

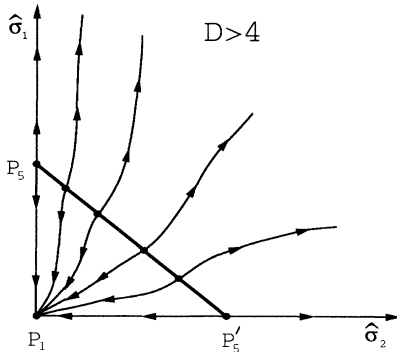


FIG. 4. Flow diagram for $D > 4$ in $T=0$ subspace. The critical exponents are constant along the line of fixed points stretching from P_5 to P'_5 fixed points.

value defined by $\hat{\sigma}_{\text{eff}}^*$, the flat phase of the membrane becomes unstable and the flows again head toward the strong disorder phase, outside the range of validity of the ϵ expansion.

We find that the critical exponents are *constant* along the line of fixed points (see below), so that the direction along the line represents a redundant operator. This redundancy arises because only the special, elastic-constant-dependent combination of parameters (4.8) appears in the $T=0$ recursion relations to one-loop order. When $D=2$ this combination is just $(\sigma_1 + \sigma_2)K_0^2$, which is the combination determining the renormalization of the bending rigidity in Eq. (3.7).

We use the scaling relations Eq. (4.7) to compute the singular dependence of κ_R , μ_R , and $2\mu_R + \lambda_R$ on the disorder $\hat{\sigma}_{\text{eff}} - \hat{\sigma}_{\text{eff}}^*$ at $T=0$. The η exponents are obtained by evaluating the scaling functions defined in Eqs. (4.3) on the fixed line, giving $\eta_{\kappa}(P_5) = -|\epsilon|/2$ and $\eta_{\perp}(P_5) = \eta_{\parallel}(P_5) = 0$. The eigenvalue in the direction of increasing disorder is computed in Appendix C with the result $y_{\sigma} = |\epsilon|$. In Eqs. (4.7) we rescale well outside the critical region by choosing $l=l^*$ such that $\hat{\sigma}_{\text{eff}}(l^*) - \hat{\sigma}_{\text{eff}}^* = e^{l^*}(\hat{\sigma}_{\text{eff}} - \hat{\sigma}_{\text{eff}}^*) = 1$. This then leads to a vanishing renormalized bending rigidity

$$\kappa_R \sim (\hat{\sigma}_{\text{eff}} - \hat{\sigma}_{\text{eff}}^*)^{1/2 + O(\epsilon)}. \quad (4.9)$$

We also find that the renormalized Lamé coefficients are nonuniversal finite constants at $T=0$. We shall argue in Sec. V that the transition for $\hat{\sigma}_{\text{eff}} > \hat{\sigma}_{\text{eff}}^*$ is to a highly degenerate spin-glass-like ground state.

The flows at finite temperature for $D > 4$ are indicated schematically in Fig. 5 where we projected down onto an attractive invariant subspace $\hat{\mu} = -3\hat{\lambda}$. The instability toward strong disorder still requires a certain threshold strength defined by a two-dimensional “transition surface” (see Appendix C). This surface in the $\hat{\mu}, \hat{\sigma}_1, \hat{\sigma}_2$ space, terminating at $\hat{\sigma}_{\text{eff}}^*$, divides the parameter space into the pure and disorder-dominated regions. At low temperatures the disorder threshold value $\hat{\sigma}_{\text{eff}}^*(\hat{\mu})$ increases linearly with $\hat{\mu}$, leading to a planar “transition surface.” However, because P_5 is repulsive in temperature as well as disorder direction, this fixed point does not

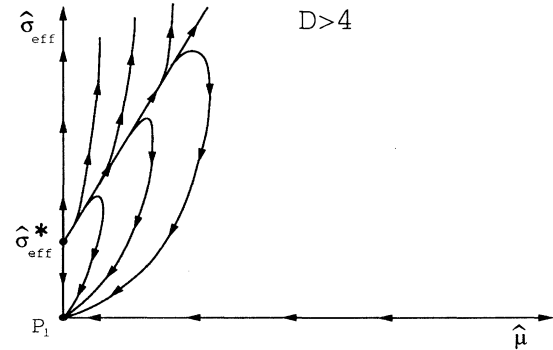


FIG. 5. Flow diagram for $D > 4$ illustrating the finite threshold (order ϵ) of disorder needed to activate the instability at all temperatures.

control the transition at finite temperatures. It is likely that there is a finite-temperature nonperturbative critical fixed point further out the “transition surface” that controls the transition. Other methods must be used to study the transition at finite temperature [21].

V. SUMMARY AND SPECULATIONS ON SPIN-GLASS ORDER

In the absence of disorder, phantom polymerized membranes undergo a phase transition between a crumpled and a flat phase as the temperature is lowered. The flat phase is remarkable because its lower critical dimension is less than 2, even though it is a continuous symmetry that is being broken. What makes this possible is the nonlinear coupling between the in-plane and out-of-plane fluctuations, which leads to a diverging bending rigidity under renormalization.

In this paper we have shown that this flat phase is actually rather fragile, at least when quenched disorder is present. The effects of impurities and other imperfections were modeled by random deformations in the metric of the lowest-energy configuration of the membrane. At low temperatures, disorder generically leads to the breakdown of the flat phase. If unbound disclinations are included in the disorder, this breakdown occurs at *all* temperatures.

We have several reasons to believe that these instabilities lead to spin-glass phases:

(i) Above $D=4$, and for arbitrary $d_c = d - D$, we can increase the disorder $\hat{\sigma}_{\text{eff}}$ to its critical value $\hat{\sigma}_{\text{eff}}^c$. The zero-temperature bending rigidity vanishes rapidly as $\hat{\sigma}_{\text{eff}} \rightarrow \hat{\sigma}_{\text{eff}}^c$ from below, while Lamé coefficients approach constant values [see Eq. (4.9)]. These results hint that the phase above this threshold is dominated by many highly crumpled, degenerate configurations, because of the vanishing bending rigidity. The barriers (typically requiring stretching nearest-neighbor bonds) separating these configurations, however, may be quite high (as in a spin glass), as suggested by the finiteness of the Lamé coefficients near the transition.

(ii) There are indications that a spin-glass phase (with Edwards-Anderson order in the surface tangents) exists in the exactly soluble limit $d \rightarrow \infty$ [21]. The phase diagrams suggested by this approach are just what we have conjectured based on the ϵ expansions.

(iii) For the special case of $d=3$ and $D=2$ we can argue as follows [20]. To interpret the softening of the bending rigidity displayed in Eq. (3.7), we consider the problem of minimizing the effective free energy in Eq. (3.5). If the renormalized bending rigidity is indeed small, it makes sense to proceed by determining first the smallest possible value of the elastic stretching energy. This is given by the solution of $\frac{1}{2}P_{\alpha\beta}^T(\partial_{\alpha}f)(\partial_{\beta}f) = P_{\alpha\beta}^T c_{\alpha\beta}(\mathbf{x})$, or equivalently (upon taking the Laplacian)

$$S(\mathbf{x}) = (\partial_1^2 f)(\partial_2^2 f) - (\partial_1 \partial_2 f)^2 = -\nabla^2 P_{\alpha\beta}^T c_{\alpha\beta}(\mathbf{x}), \quad (5.1)$$

where $S(\mathbf{x})$ is the Gaussian curvature. There are, in general, many configurations that minimize the stretching energy, adapting themselves to the frozen-in distribution

of impurity disorder. The true ground states are given by those solutions that also minimize the bending energy. The softening of the bending rigidity displayed in Eq. (3.7) suggests that these different long-wavelength configurations, which minimize the elastic energy, will be nearly degenerate.

The degeneracy of these competing minima is, in fact, Ising-like. Consider, for example, a single large impurity atom that causes an otherwise flat membrane to pucker up or down, reflecting the invariance of solutions to Eq. (5.1) to the transformation $f \rightarrow -f$. Puckering will screen the elastic interaction between a collection of well-separated impurities. The weakly interacting two-level systems embodied in this picture are reminiscent of an Ising spin glass. One might expect that the bending energy induces an “antiferromagnetic” interaction (i.e., it prefers puckers on opposite sides of the membrane) between these two-level systems, especially when distant self-avoidance is present. The interaction between elastic dipoles (e.g., well-separated long bonds), on the other hand, could be either ferromagnetic or antiferromagnetic, depending on their relative orientation. We expect a diverging Edwards-Anderson correlation length associated with these puckers as $T \rightarrow 0$, as has been found in extensive numerical simulations in the two-dimensional Ising spin glass [38].

Ising spin-glass order in the puckers could lead to a “roughened” but flat glassy phase, quite different from the crumpled spin glass proposed for phantom membranes as $d \rightarrow \infty$ [21]. Sorting out exactly what happens as a function of d and D and when self-avoidance is included are important subjects for future investigations.

ACKNOWLEDGMENTS

This work was supported by the National Science Foundation through Grant No. DMR-88-17291, and through the Harvard Materials Research Laboratory. One of us (L.R.) acknowledges support by the Hertz Foundation. We thank Y. Kantor for providing us with Fig. 1(c). It is a pleasure to acknowledge helpful discussions with F. F. Abraham, D. Bensimon, R. R. Chianelli, D. S. Fisher, E. Frey, D. Huse, P. Le Doussal, and T. C. Lubensky.

APPENDIX A: CALCULATION OF β FUNCTIONS AND CRITICAL EXPONENTS

In this appendix we provide the details of the one-loop calculation of the renormalized coupling constants, fixed points, and the critical exponents. The low-temperature flat phase of the membrane is described by the effective Hamiltonian Eq. (3.2), generalized to D -dimensional manifolds embedded in d dimensions,

$$\beta\mathcal{F}_{\text{eff}}[\vec{f}, u_{\alpha}, c_{\alpha\beta}] = \int d^D x \left[\frac{1}{2} \kappa (\partial_{\alpha}^2 \vec{f})^2 + \mu (u_{\alpha\beta}^0)^2 + \frac{1}{2} \lambda (u_{\alpha\alpha}^0)^2 - 2\mu c_{\alpha\beta} u_{\alpha\beta}^0 - \lambda c_{\beta\beta} u_{\alpha\alpha}^0 \right]. \quad (A1)$$

In this appendix we have for convenience absorbed the factor $\beta = 1/k_B T$ in κ , μ , and λ . Upon using Eq. (3.3) we obtain

$$\begin{aligned}
\beta \mathcal{F}_{\text{eff}}[\vec{f}, u_\alpha, c_{\alpha\beta}] = \int d^D x \{ & \frac{1}{2} \kappa (\partial_\alpha^2 \vec{f})^2 - \frac{1}{2} u_\alpha \nabla^2 [\mu P_{\alpha\beta}^T + (2\mu + \lambda) P_{\alpha\beta}^L] u_\beta \\
& + \frac{1}{4} \mu (\partial_\alpha \vec{f} \cdot \partial_\beta \vec{f})^2 + \frac{1}{8} \lambda (\partial_\alpha \vec{f} \cdot \partial_\alpha \vec{f})^2 + \mu (\partial_\alpha u_\beta) (\partial_\alpha \vec{f}) \cdot (\partial_\beta \vec{f}) \\
& + \frac{1}{2} (\partial_\alpha u_\alpha) (\partial_\beta \vec{f}) \cdot (\partial_\beta \vec{f}) - 2\mu (\partial_\alpha u_\beta) c_{\alpha\beta} - \mu (\partial_\alpha \vec{f}) \cdot (\partial_\beta \vec{f}) c_{\alpha\beta} \\
& - \lambda (\partial_\alpha u_\alpha) c_{\beta\beta} - \frac{1}{2} \lambda (\partial_\alpha \vec{f}) \cdot (\partial_\alpha \vec{f}) c_{\beta\beta} \}, \tag{A2}
\end{aligned}$$

where $P_{\alpha\beta}^T$ and $P_{\alpha\beta}^L$ are transverse and longitudinal projection operators

$$P_{\alpha\beta}^T = \delta_{\alpha\beta} - \frac{\partial_\alpha \partial_\beta}{\nabla^2}, \tag{A3a}$$

$$P_{\alpha\beta}^L = \frac{\partial_\alpha \partial_\beta}{\nabla^2}. \tag{A3b}$$

The averages over the annealed field $\vec{f}(\mathbf{x})$ and $u_\alpha(\mathbf{x})$ are taken with the usual Boltzmann weight factor with the quenched field $c_{\alpha\beta}(\mathbf{x})$ fixed. Then the quenched average of only the connected diagrams is performed, with a weight $\mathcal{P}[c_{\alpha\beta}(\mathbf{x})]$ from Eq. (2.9).

From the Fourier transform of the Hamiltonian in Eq. (A2) we can read off the Feynman rules in momentum space. The propagators for $\vec{f}(\mathbf{k})$, $u_\alpha(\mathbf{k})$, and $c_{\alpha\beta}(\mathbf{k})$ are

$$\langle f_i f_j \rangle_0 = \frac{\delta_{ij}}{\kappa |\mathbf{k}|^4}, \tag{A4a}$$

$$\langle u_\alpha u_\beta \rangle_0 = \frac{P_{\alpha\beta}^T}{\mu |\mathbf{k}|^2} + \frac{P_{\alpha\beta}^L}{(2\mu + \lambda) |\mathbf{k}|^2}, \tag{A4b}$$

$$\begin{aligned}
\overline{c_{\alpha\beta} c_{\gamma\delta}} = & (\sigma_1 - \sigma_2 / D) \delta_{\alpha\beta} \delta_{\gamma\delta} \\
& + \frac{1}{2} \sigma_2 (\delta_{\alpha\gamma} \delta_{\beta\delta} + \delta_{\alpha\delta} \delta_{\beta\gamma}), \tag{A4c}
\end{aligned}$$

symbolized by a solid, wavy, and dotted lines, respectively. The vertices are listed in Fig. 6 and defined analytically by the tree-level correlation functions

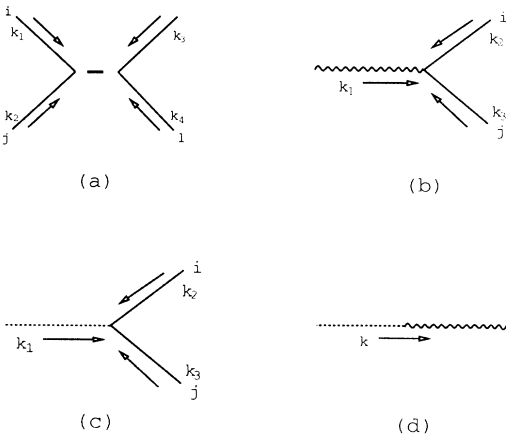


FIG. 6. Vertices of the Hamiltonian in Eq. (A2).

$$\begin{aligned}
& \langle [f_i(\mathbf{k}_1) f_j(\mathbf{k}_2)] [f_k(\mathbf{k}_3) f_l(\mathbf{k}_4)] \rangle_0 \\
& = \frac{\mu}{4} (\mathbf{k}_1 \cdot \mathbf{k}_2) (\mathbf{k}_3 \cdot \mathbf{k}_4) \delta_{ik} \delta_{jl} + \frac{\lambda}{8} (\mathbf{k}_1 \cdot \mathbf{k}_2) (\mathbf{k}_3 \cdot \mathbf{k}_4) \delta_{ij} \delta_{kl}, \tag{A5a}
\end{aligned}$$

$$\begin{aligned}
& \langle u_\alpha(\mathbf{k}_1) f_i(\mathbf{k}_2) f_j(\mathbf{k}_3) \rangle_0 \\
& = -\frac{i}{2} \{ \mu [k_{3\alpha} (\mathbf{k}_1 \cdot \mathbf{k}_2) + k_{2\alpha} (\mathbf{k}_1 \cdot \mathbf{k}_3)] \\
& \quad + \lambda k_{1\alpha} (\mathbf{k}_2 \cdot \mathbf{k}_3) \} \delta_{ij}, \tag{A5b}
\end{aligned}$$

$$\langle u_\alpha(\mathbf{k}) \rangle_0 = -i (2\mu k_\beta c_{\alpha\beta} + \lambda k_\alpha c_{\beta\beta}), \tag{A5c}$$

$$\langle f_i(\mathbf{k}_1) f_j(\mathbf{k}_2) \rangle_0 = [\mu k_{1\alpha} k_{2\beta} c_{\alpha\beta} + \frac{1}{2} \lambda (\mathbf{k}_1 \cdot \mathbf{k}_2) c_{\alpha\alpha}] \delta_{ij}. \tag{A5d}$$

Following the original ideas of Wilson and Kogut [39] we implement the momentum-shell renormalization-group transformation. We integrate out all the fields with $b^{-1}\Lambda < |\mathbf{k}| < \Lambda$, $b > 1$ and rescale the remaining degrees of freedom:

$$\mathbf{k} = \mathbf{k}' / b, \tag{A6a}$$

$$\vec{f}(\mathbf{k}) = b^{\xi_f} \vec{f}'(\mathbf{k}'), \tag{A6b}$$

$$u_\alpha^T(\mathbf{k}) = b^{\xi_\perp} u_\alpha^T(\mathbf{k}'), \tag{A6c}$$

$$u_\alpha^L(\mathbf{k}) = b^{\xi_\parallel} u_\alpha^L(\mathbf{k}'), \tag{A6d}$$

$$c_{\alpha\beta}(\mathbf{k}) = b^{\xi_c} c'_{\alpha\beta}(\mathbf{k}'). \tag{A6e}$$

This transformation maps the original theory characterized by the set of parameters $\{\kappa, \mu, \lambda, \sigma_1, \sigma_2\}$ onto a theory described by a new set of coupling constants $\{\kappa(b), \mu(b), \lambda(b), \sigma_1(b), \sigma_2(b)\}$. The relation between the coupling constants is determined by the appropriate correlation functions computed perturbatively. The Ward identities associated with the $O(d)$ symmetry ensure that the coupling constants renormalize in the same way, regardless of which vertex is used to define them. $O(d)$ invariance also leads to a relation between the rescaling of $\vec{f}(\mathbf{k})$, $u_\alpha^T(\mathbf{k})$, and $u_\alpha^L(\mathbf{k})$,

$$\xi_\perp = \xi_\parallel = 2\xi_f - D - 1, \tag{A7}$$

which leads to the relation between the scaling exponents η_κ , η_\perp , and η_\parallel introduced in Eqs. (4.1) of the main text (see below) [8]. We have checked that these Ward identities are satisfied to one-loop order. The one-loop correction to the phonon propagator $\langle u_\alpha(\mathbf{k}) u_\beta(-\mathbf{k}) \rangle_c$ is displayed in Fig. 7 and leads to recursion relations

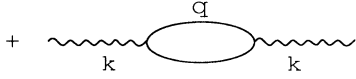


FIG. 7. One-loop correction to the in-plane phonon propagator.

$$\mu'(b) = \mu b^{2\xi_1 - D - 2} \left[1 - \frac{2d_c}{D^2 + 2D} \frac{\mu}{\kappa^2} A_D \int_{1/b}^1 \frac{q^{D-1}}{|q|^4} dq \right], \quad (\text{A8a})$$

$$(2\mu + \lambda)'(b) = (2\mu + \lambda) b^{2\xi_1 - D - 2} \times \left[1 - d_c \frac{6\mu^2 + 2\mu\lambda(D+2) + \lambda^2(D^2 + 2D)/2}{(2\mu + \lambda)\kappa^2(D^2 + 2D)} \times A_D \int_{1/b}^1 \frac{q^{D-1}}{|q|^4} dq \right], \quad (\text{A8b})$$

where A_D is related to the surface area S_D of a D -dimensional sphere and $d_c = d - D$. Similarly, the one-loop renormalization of the phonon-disorder correlation function $\langle u_\beta(\mathbf{k})c_{\alpha\beta}(-\mathbf{k}) \rangle_c$ is depicted in Fig. 8 and leads to recursion relations for the disorder fields $\hat{c}_{\alpha\beta}$ and $c_{\alpha\alpha}$

$$[(2\mu + D\lambda)c_{\alpha\alpha}]'(b) = [(2\mu + D\lambda)c_{\alpha\alpha}] b^{\xi_1 - D - 1} \times \left[1 - \frac{d_c}{2D} \frac{2\mu + D\lambda}{\kappa^2} \times A_D \int_{1/b}^1 \frac{q^{D-1}}{|q|^4} dq \right], \quad (\text{A9a})$$

$$(2\mu\hat{c}_{\alpha\beta})'(b) = (2\mu\hat{c}_{\alpha\beta}) b^{\xi_1 - D - 1} \times \left[1 - \frac{2d_c}{D^2 + 2D} \frac{\mu}{\kappa^2} A_D \int_{1/b}^1 \frac{q^{D-1}}{|q|^4} dq \right]. \quad (\text{A9b})$$

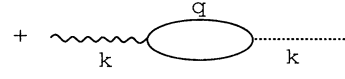


FIG. 8. One-loop correction to the phonon-disorder correlation function.

Equations (A9a) and (A9b) in turn lead to the renormalization of $\hat{\sigma}_1$ and $\hat{\sigma}_2$ by reexpressing the quenched probability distribution $\mathcal{P}[c_{\alpha\beta}]$ in terms of $c'_{\alpha\alpha}$ and $\hat{c}'_{\alpha\beta}$ and identifying the new variances as σ'_1 and σ'_2 . Because in the expression for renormalization of κ (see below) σ_1 appears in a combination $\hat{\sigma}_1 = A_D [2\mu(2\mu + D\lambda)/(2\mu + \lambda)]^2 \sigma_1/\kappa^2$, we recast the recursion relations in terms of this variable. It is also convenient to define $\hat{\sigma}_2 = A_D (2\mu)^2 \sigma_2/\kappa^2$. The recursion relations for $\hat{\sigma}_1$ and $\hat{\sigma}_2$ are

$$\hat{\sigma}'_1(b) = \hat{\sigma}_1 \left[\frac{\kappa}{\kappa'} \right]^2 b^{2\xi_1 - D - 2} \times \left[1 - \frac{2d_c}{\kappa^2} \frac{D+1}{D^2 + 2D} \frac{\mu(2\mu + D\lambda)}{2\mu + \lambda} \times A_D \int_{1/b}^1 \frac{q^{D-1}}{|q|^4} dq \right], \quad (\text{A10a})$$

$$\hat{\sigma}'_2(b) = \hat{\sigma}_2 \left[\frac{\kappa}{\kappa'} \right]^2 b^{2\xi_1 - D - 2} \times \left[1 - \frac{4d_c}{D^2 + 2D} \frac{\mu}{\kappa^2} A_D \int_{1/b}^1 \frac{q^{D-1}}{|q|^4} dq \right]. \quad (\text{A10b})$$

The renormalized κ_R can be more simply calculated by first integrating out the u_α degrees of freedom (as in Sec. III), leading to an effective Hamiltonian involving only $c_{\alpha\beta}(\mathbf{k})$ and $\vec{f}(\mathbf{k})$,

$$\beta\mathcal{F}_{\text{eff}}[\vec{f}, c_{\alpha\beta}] = \frac{\kappa}{2} \int_{\mathbf{k}} |\mathbf{k}|^4 |\vec{f}(\mathbf{k})|^2 + \frac{1}{8} \int_{\mathbf{k}_1} \int_{\mathbf{k}_2} \int_{\mathbf{k}_3} \left[2\mu P_{\alpha\gamma}^T P_{\beta\delta}^T(\mathbf{q}) + \frac{2\mu\lambda}{2\mu + \lambda} P_{\alpha\beta}^T P_{\gamma\delta}^T(\mathbf{q}) \right] \times k_{1\alpha} k_{2\beta} k_{3\gamma} k_{4\delta} [\vec{f}(\mathbf{k}_1) \cdot \vec{f}(\mathbf{k}_2)] [\vec{f}(\mathbf{k}_3) \cdot \vec{f}(\mathbf{k}_4)] + \frac{1}{2} \int_{\mathbf{k}_1} \int_{\mathbf{k}_2} \left[2\mu P_{\alpha\gamma}^T P_{\beta\delta}^T(\mathbf{q}) + \frac{2\mu\lambda}{2\mu + \lambda} P_{\alpha\beta}^T P_{\gamma\delta}^T(\mathbf{q}) \right] k_{1\alpha} k_{2\beta} c_{\gamma\delta}(\mathbf{q}) \vec{f}(\mathbf{k}_1) \cdot \vec{f}(\mathbf{k}_2). \quad (\text{A11})$$

Here $\mathbf{q} = -\mathbf{k}_1 - \mathbf{k}_2$ in the third term, and $\mathbf{k}_1 + \mathbf{k}_2 + \mathbf{k}_3 + \mathbf{k}_4 = \mathbf{0}$ in the second. Also for shorthand we define $\int_{\mathbf{k}} \equiv 1/(2\pi)^D \int d^D k$.

This Hamiltonian leads to the Feynman rules for the calculation of \vec{f} correlation functions quenched averaged over $c_{\alpha\beta}$. The propagator is given by Eq. (A4a), and the effective vertices are displayed in Fig. 9 and defined analytically by

$$\overline{\langle f_i(\mathbf{k}_1) f_j(\mathbf{k}_2) f_k(\mathbf{k}_3) f_l(\mathbf{k}_4) \rangle_c} = \frac{1}{8} \delta_{ij} \delta_{kl} \left[2\mu P_{\alpha\gamma}^T P_{\beta\delta}^T(\mathbf{q}) + \frac{2\mu\lambda}{2\mu + \lambda} P_{\alpha\beta}^T P_{\gamma\delta}^T(\mathbf{q}) \right] k_{1\alpha} k_{2\beta} k_{3\gamma} k_{4\delta}, \quad (\text{A12a})$$

$$\overline{\langle f_i(\mathbf{k}_1) f_j(\mathbf{k}_2) \rangle_c} = \frac{1}{2} \delta_{ij} \left[2\mu P_{\alpha\gamma}^T P_{\beta\delta}^T(\mathbf{q}) + \frac{2\mu\lambda}{2\mu + \lambda} P_{\alpha\beta}^T P_{\gamma\delta}^T(\mathbf{q}) \right] c_{\alpha\beta} k_{1\gamma} k_{2\delta}. \quad (\text{A12b})$$

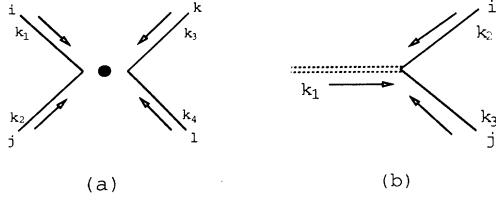


FIG. 9. Vertices of the effective theory described by the effective Hamiltonian in Eq. (A11), obtained by integrating out the in-plane phonon modes.

These Feynman rules lead to the renormalization of κ , defined in terms of $\overline{\langle f_i(\mathbf{k})f_j(-\mathbf{k}) \rangle}_c$. The diagrams contributing to the corrections of the tree-level result are shown in Fig. 10 and lead to the recursion relation for κ

$$\kappa'(b) = \kappa b^{2\xi_f - D - 4} \left[1 + \frac{D^2 - 1}{D^2 + 2D} \left\{ \frac{4\mu(\mu + \lambda)}{\kappa^2(2\mu + \lambda)} A_D - \hat{\sigma}_1 - \hat{\sigma}_2 \left[\frac{D-1}{D} \left[\frac{2\mu}{2\mu + \lambda} \right]^2 + \frac{2\lambda}{2\mu + \lambda} \right] \right\} \int_{1/b}^1 \frac{q^{D-1}}{|q|^4} dq \right]. \quad (\text{A13})$$

We make implicit choice of ξ_f by requiring κ to be a renormalization-group invariant $\kappa'(b) = \kappa$. This choice leads to

$$2\xi_f - D - 4 = - \frac{D^2 - 1}{D^2 + 2D} \left\{ \frac{4\mu(\mu + \lambda)}{\kappa^2(2\mu + \lambda)} A_D - \hat{\sigma}_1 - \hat{\sigma}_2 \left[\frac{D-1}{D} \left[\frac{2\mu}{2\mu + \lambda} \right]^2 + \frac{2\lambda}{2\mu + \lambda} \right] \right\}. \quad (\text{A14})$$

We observe that in Eq. (A13) the true coupling constants of the expansion are $\hat{\mu} = A_D \mu / \kappa^2$, $\hat{\lambda} = A_D \lambda / \kappa^2$, and the reduced disorder strengths $\hat{\sigma}_1 = A_D [2\mu(2\mu + D\lambda) / (2\mu + \lambda)]^2 \sigma_1 / \kappa^2$, $\hat{\sigma}_2 = A_D (2\mu)^2 \sigma_2 / \kappa^2$. Equations (A8a), (A8b), (A10a), and (A10b), together with Eq. (A7) then lead to the recursion relations for these effective coupling constants in $D = 4 - \epsilon$ dimensions,

$$\hat{\mu}'(b) = \hat{\mu} b^{4\xi_f - 3D - 4} \left[1 - \frac{d_c}{12} \hat{\mu} \ln b \right], \quad (\text{A15a})$$

$$\hat{\lambda}'(b) = \hat{\lambda} b^{4\xi_f - 3D - 4} \left[1 - \frac{d_c}{12} (\hat{\mu}^2 + 6\hat{\mu}\hat{\lambda} + 6\hat{\lambda}^2) \ln b \right], \quad (\text{A15b})$$

$$\hat{\sigma}_1'(b) = \hat{\sigma}_1 b^{4\xi_f - 3D - 4} \left[1 - \frac{5}{6} d_c \frac{\hat{\mu}(\hat{\mu} + 2\hat{\lambda})}{2\hat{\mu} + \hat{\lambda}} \ln b \right], \quad (\text{A15c})$$

$$\hat{\sigma}_2'(b) = \hat{\sigma}_2 b^{4\xi_f - 3D - 4} \left[1 - \frac{d_c}{6} \hat{\mu} \ln b \right]. \quad (\text{A15d})$$

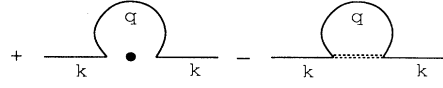


FIG. 10. These diagrams are the one-loop corrections to the renormalization of κ . The opposite signs of the two contributions are in competition. The second disorder term wins at low temperatures, leading to the instability of the flat phase.

These recursion relations, upon differentiation with respect to $\ln b$ and using Eq. (A14), lead to the β functions quoted in the Eqs. (4.4a)–(4.4d) and determine the renormalization-group flow with fixed points as the zeros of the β functions.

We now relate the ξ_f , ξ_\perp , and ξ_\parallel functions to the scaling exponents defined in Eqs. (4.1) of the main text. We have already determined ξ_f , Eq. (A14). Similar definitions of ξ_\perp and ξ_\parallel lead to

These recursion relations, upon differentiation with respect to $\ln b$ and using Eq. (A14), lead to the β functions quoted in the Eqs. (4.4a)–(4.4d) and determine the renormalization-group flow with fixed points as the zeros of the β functions.

We now relate the ξ_f , ξ_\perp , and ξ_\parallel functions to the scaling exponents defined in Eqs. (4.1) of the main text. We have already determined ξ_f , Eq. (A14). Similar definitions of ξ_\perp and ξ_\parallel lead to

$$2\xi_\perp - D - 2 = A_D \frac{2d_c}{D^2 + 2D} \frac{\mu}{\kappa^2}, \quad (\text{A16a})$$

$$2\xi_\parallel - D - 2 = A_D d_c \frac{6\mu^2 + 2\mu\lambda(D+2) + \lambda^2(D^2 + 2D)/2}{(2\mu + \lambda)\kappa^2(D^2 + 2D)}. \quad (\text{A16b})$$

Using Eqs. (A6) we derive the renormalization-group transformations for the correlation functions that define κ_R , μ_R , and $2\mu_R + \lambda_R$:

$$\overline{\langle |f(\mathbf{k})|^2 \rangle}_c = b^{2\xi_f - D} \overline{\langle |f(b\mathbf{k})|^2 \rangle}_c, \quad (\text{A17a})$$

$$\overline{\langle u_\alpha^T(\mathbf{k})u_\beta^T(-\mathbf{k}) \rangle}_c = b^{2\xi_\perp - D} \overline{\langle u_\alpha^T(b\mathbf{k})u_\beta^T(-b\mathbf{k}) \rangle}_c, \quad (\text{A17b})$$

$$\overline{\langle u_\alpha^L(\mathbf{k})u_\beta^L(-\mathbf{k}) \rangle}_c = b^{2\xi_\parallel - D} \overline{\langle u_\alpha^L(b\mathbf{k})u_\beta^L(-b\mathbf{k}) \rangle}_c, \quad (\text{A17c})$$

where the extra factor of b^{-D} comes from the rescaling of the momentum-conserving δ function implicit in the definition of the average. We choose $b = b^*$ such that $b^*|\mathbf{k}| = 1$ and obtain

$$\overline{\langle |f(\mathbf{k})|^2 \rangle_c} = |\mathbf{k}|^{-2\xi_f + D} \overline{\langle |f(1)|^2 \rangle_c}, \quad (\text{A18a})$$

$$\overline{\langle u_\alpha^T(\mathbf{k}) u_\beta^T(-\mathbf{k}) \rangle_c} = |\mathbf{k}|^{-2\xi_1 + D} \overline{\langle u_\alpha^T(1) u_\beta^T(-1) \rangle_c}, \quad (\text{A18b})$$

$$\overline{\langle u_\alpha^L(\mathbf{k}) u_\beta^L(-\mathbf{k}) \rangle_c} = |\mathbf{k}|^{-2\xi_{\parallel} + D} \overline{\langle u_\alpha^L(1) u_\beta^L(-1) \rangle_c}. \quad (\text{A18c})$$

Using Eqs. (4.1), which define κ_R , μ_R , and $2\mu_R + \lambda_R$ in terms of the above correlation functions, we obtain

$$\eta_\kappa = -2\xi_f + D + 4, \quad (\text{A19a})$$

$$\eta_{\perp} = 2\xi_{\perp} - D - 2, \quad (\text{A19b})$$

$$\eta_{\parallel} = 2\xi_{\parallel} - D - 2. \quad (\text{A19c})$$

Together with Eq. (A7) these equations lead to the relation between the scaling exponents

$$\mu(-\epsilon + \eta_{\perp} + 2\eta_\kappa) = (2\mu + \lambda)(-\epsilon + \eta_{\parallel} + 2\eta_\kappa) = 0. \quad (\text{A20})$$

Finally, using the expression for ξ_f , ξ_{\perp} , and ξ_{\parallel} in Eqs. (A19), we obtain

$$\eta_\kappa = \frac{5}{8} \left[\frac{4\hat{\mu}(\hat{\mu} + \hat{\lambda})}{2\hat{\mu} + \hat{\lambda}} - \hat{\sigma}_1 - \hat{\sigma}_2 \left[\frac{3\hat{\mu}^2}{(2\hat{\mu} + \hat{\lambda})^2} + \frac{2\hat{\lambda}}{2\hat{\mu} + \hat{\lambda}} \right] \right], \quad (\text{A21a})$$

$$\eta_{\perp} = \frac{d_c}{12} \hat{\mu}, \quad (\text{A21b})$$

$$\eta_{\parallel} = d_c \frac{\hat{\mu}^2 + 2\hat{\mu}\hat{\lambda} + 2\hat{\lambda}^2}{4(2\hat{\mu} + \hat{\lambda})}. \quad (\text{A21c})$$

These functions, when evaluated at the relevant fixed points, lead to the scaling exponents in Sec. IV of the main text.

APPENDIX B: REPLICIA METHOD

In this appendix we will rederive the recursion relations using the replica method [40] as an independent check on the calculations in Appendix A. To calculate the renormalization of κ within the replica formalism it is again convenient to work with the effective free energy in which the phonon degrees of freedom have been integrated out exactly. As usual [40], we introduce n copies of fields \vec{f} labeled by an index a with a total free energy given by the replicated version of the free energy Eq. (A11),

$$\begin{aligned} \beta \mathcal{F}_{\text{eff}}^r[\vec{f}_a, c_{\alpha\beta}] = & \sum_{a=1}^n \left[\frac{\kappa}{2} \int_{\mathbf{k}} |\mathbf{k}|^4 |\vec{f}_a(\mathbf{k})|^2 + \frac{1}{8} \int_{k_1} \int_{k_2} \int_{k_3} \left[2\mu P_{\alpha\gamma}^T P_{\beta\delta}^T(\mathbf{q}) + \frac{2\mu\lambda}{2\mu + \lambda} P_{\alpha\beta}^T P_{\gamma\delta}^T(\mathbf{q}) \right] \right. \\ & \times k_{1\alpha} k_{2\beta} k_{3\gamma} k_{4\delta} [\vec{f}_a(\mathbf{k}_1) \cdot \vec{f}_a(\mathbf{k}_2)] [\vec{f}_a(\mathbf{k}_3) \cdot \vec{f}_a(\mathbf{k}_4)] \\ & \left. + \frac{1}{2} \int_{k_1} \int_{k_2} \left[2\mu P_{\alpha\gamma}^T P_{\beta\delta}^T(\mathbf{q}) + \frac{2\mu\lambda}{2\mu + \lambda} P_{\alpha\beta}^T P_{\gamma\delta}^T(\mathbf{q}) \right] k_{1\alpha} k_{2\beta} c_{\gamma\delta}(\mathbf{q}) \vec{f}_a(\mathbf{k}_1) \cdot \vec{f}_a(\mathbf{k}_2) \right]. \quad (\text{B1}) \end{aligned}$$

Assuming that it is possible to interchange the thermodynamic limit and the limit $n \rightarrow 0$, the equivalence of the original theory with a quenched field $c_{\alpha\beta}$ and the replicated theory (in the limit $n \rightarrow 0$) with only annealed fields is established through the identity

$$\ln Z = \lim_{n \rightarrow 0} \frac{Z^n - 1}{n}. \quad (\text{B2})$$

To compute the κ_R we can integrate out $c_{\alpha\beta}$ exactly, since it only enters quadratically and linearly. The final free energy then contains n annealed coupled \vec{f}_a fields:

$$\begin{aligned} \beta \mathcal{F}_{\text{eff}}^r[\vec{f}_a] = & \sum_{a=1}^n \left[\frac{\kappa}{2} \int_{\mathbf{k}} |\mathbf{k}|^4 |\vec{f}_a(\mathbf{k})|^2 + \sum_{a=1}^n \frac{1}{8} \int_{k_1} \int_{k_2} \int_{k_3} \left[2\mu P_{\alpha\gamma}^T P_{\beta\delta}^T(\mathbf{q}) + \frac{2\mu\lambda}{2\mu + \lambda} P_{\alpha\beta}^T P_{\gamma\delta}^T(\mathbf{q}) \right] \right. \\ & \times k_{1\alpha} k_{2\beta} k_{3\gamma} k_{4\delta} [\vec{f}_a(\mathbf{k}_1) \cdot \vec{f}_a(\mathbf{k}_2)] [\vec{f}_a(\mathbf{k}_3) \cdot \vec{f}_a(\mathbf{k}_4)] \\ & \left. - \sum_{a,b} \frac{1}{8} \int_{k_1} \int_{k_2} \int_{k_3} \left[\frac{\kappa^2}{A_D} \right] \left[\hat{\sigma}_1 P_{\alpha\beta}^T P_{\gamma\delta}^T(\mathbf{q}) + \hat{\sigma}_2 \left[P_{\alpha\gamma}^T P_{\beta\delta}^T(\mathbf{q}) + \frac{\lambda^2 - 4\mu^2/D}{(2\mu + \lambda)^2} P_{\alpha\beta}^T P_{\gamma\delta}^T(\mathbf{q}) \right] \right] \right. \\ & \left. \times k_{1\alpha} k_{2\beta} k_{3\gamma} k_{4\delta} [\vec{f}_a(\mathbf{k}_1) \cdot \vec{f}_a(\mathbf{k}_2)] [\vec{f}_b(\mathbf{k}_3) \cdot \vec{f}_b(\mathbf{k}_4)] \right]. \quad (\text{B3}) \end{aligned}$$

The one-loop correction to the two-point correlation function $\langle f_i^a(\mathbf{k}) f_j^a(-\mathbf{k}) \rangle_c$, which determines $\kappa'(b)$, is expressed diagrammatically in Fig. 11. Upon taking the $n \rightarrow 0$ limit, the last diagram in Fig. 11 vanishes because it is proportional to n , and we recover the result of Eq. (A13):

$$\kappa'(b) = \kappa b^{2\xi_f - D - 4} \left[1 + \frac{D^2 - 1}{D^2 + 2D} \left[\frac{4\mu(\mu + \lambda)}{\kappa^2(2\mu + \lambda)} A_D - \hat{\sigma}_1 - \hat{\sigma}_2 \left[\frac{D-1}{D} \left[\frac{2\mu}{2\mu + \lambda} \right]^2 + \frac{2\lambda}{2\mu + \lambda} \right] \right] \int_{1/b}^1 \frac{q^{D-1}}{|q|^4} dq \right]. \quad (\text{B4})$$

The renormalization of μ_R and λ_R is determined by the four-point correlation function of \vec{f}_a , diagonal in the replica indices,

$$\langle f_i^a(\mathbf{k}_1) f_i^a(\mathbf{k}_2) f_j^a(\mathbf{k}_3) f_j^a(\mathbf{k}_4) \rangle_c = \left[2\mu_R P_{\alpha\gamma}^T P_{\beta\delta}^T(\mathbf{q}) + \frac{2\mu_R \lambda_R}{2\mu_R + \lambda_R} P_{\alpha\beta}^T P_{\gamma\delta}^T(\mathbf{q}) \right] k_{1\alpha} k_{2\beta} k_{3\gamma} k_{4\delta}. \quad (\text{B5})$$

We express the renormalization of this correlation function diagrammatically in Fig. 12. In the limit of small external momenta this diagrammatic equation reduces to

$$\begin{aligned} \left[2\mu_R P_{\alpha\gamma}^T P_{\beta\delta}^T(\mathbf{q}) + \frac{2\mu_R \lambda_R}{2\mu_R + \lambda_R} P_{\alpha\beta}^T P_{\gamma\delta}^T(\mathbf{q}) \right] &= \left[2\mu P_{\alpha\gamma}^T P_{\beta\delta}^T(\mathbf{q}) + \frac{2\mu\lambda}{2\mu + \lambda} P_{\alpha\beta}^T P_{\gamma\delta}^T(\mathbf{q}) \right] \\ &\quad - \frac{d_c 2\mu^2}{\kappa^2(D^2 + 2D)} \left[P_{\alpha\beta}^T P_{\gamma\delta}^T \left[1 + \frac{\lambda^2(D^2 - 1)}{(2\mu + \lambda)^2} + \frac{2\lambda(D + 1)}{2\mu + \lambda} \right] \right. \\ &\quad \left. + 2P_{\alpha\gamma}^T P_{\beta\delta}^T \right] A_D \int_{1/b}^1 \frac{q^{D-1}}{|q|^4} dq. \end{aligned} \quad (\text{B6})$$

An independent renormalization of the $P_{\alpha\gamma}^T P_{\beta\delta}^T$ and $P_{\alpha\beta}^T P_{\gamma\delta}^T$ terms leads to the recursion relations for 2μ and $2\mu\lambda/(2\mu + \lambda)$:

$$(2\mu)'(b) = 2\mu b^{2\xi_1 - D - 2} \left[1 - \frac{d_c 2\mu}{(D^2 + 2D)\kappa^2} A_D \int_{1/b}^1 \frac{q^{D-1}}{|q|^4} dq \right], \quad (\text{B7a})$$

$$\left[\frac{2\mu\lambda}{2\mu + \lambda} \right]'(b) = \frac{2\mu\lambda}{2\mu + \lambda} b^{2\xi_1 - D - 2} \left[1 - \frac{d_c \mu}{(D^2 + 2D)\kappa^2(2\mu + \lambda)} [4\mu^2 + 4\mu\lambda(D + 2) + \lambda^2(D^2 + 2D + 2)] A_D \int_{1/b}^1 \frac{q^{D-1}}{|q|^4} dq \right]. \quad (\text{B7b})$$

Equation (B7a) agrees with Eq. (A8a). Upon using Eqs. (B7a) and (B7b) to construct a recursion relation for $2\mu + \lambda$ we recover Eq. (A8b):

$$(2\mu + \lambda)'(b) = (2\mu + \lambda) b^{2\xi_1 - D - 2} \left[1 - d_c \frac{6\mu^2 + 2\mu\lambda(D + 2) + \lambda^2(D^2 + 2D)/2}{(2\mu + \lambda)\kappa^2(D^2 + 2D)} A_D \int_{1/b}^1 \frac{q^{D-1}}{|q|^4} dq \right]. \quad (\text{B8})$$

The recursion relations for $\hat{\sigma}_1$ and $\hat{\sigma}_2$ are determined by the renormalization of the four-point function of \vec{f}_a , off diagonal in the replica index, $\langle f_i^a(\mathbf{k}_1) f_i^a(\mathbf{k}_2) f_j^b(\mathbf{k}_3) f_j^b(\mathbf{k}_4) \rangle_c$. The diagrammatic equation is displayed in Fig. 13. In the limit of vanishing external momenta and $n \rightarrow 0$, only the last two diagrams survive, and we recover the recursion relations of Eqs. (A10):

$$\begin{aligned} \hat{\sigma}_1'(b) &= \hat{\sigma}_1 \left[\frac{\kappa}{\kappa'} \right]^2 b^{2\xi_1 - D - 2} \\ &\quad \times \left[1 - \frac{2d_c}{\kappa^2} \frac{D + 1}{D^2 + 2D} \frac{\mu(2\mu + D\lambda)}{2\mu + \lambda} \right. \\ &\quad \left. \times A_D \int_{1/b}^1 \frac{q^{D-1}}{|q|^4} dq \right], \end{aligned} \quad (\text{B9a})$$

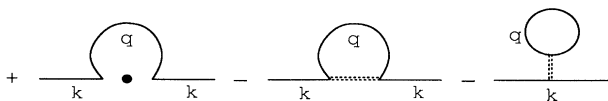


FIG. 11. One-loop corrections to the two-point correlation function of f_i^a which lead to the renormalization of κ within the replica scheme. The last term is proportional to n and hence vanishes in the limit $n \rightarrow 0$.

$$\begin{aligned} \hat{\sigma}_2'(b) &= \hat{\sigma}_2 \left[\frac{\kappa}{\kappa'} \right]^2 b^{2\xi_1 - D - 2} \\ &\quad \times \left[1 - \frac{4d_c}{D^2 + 2D} \frac{\mu}{\kappa^2} A_D \int_{1/b}^1 \frac{q^{D-1}}{|q|^4} dq \right]. \end{aligned} \quad (\text{B9b})$$

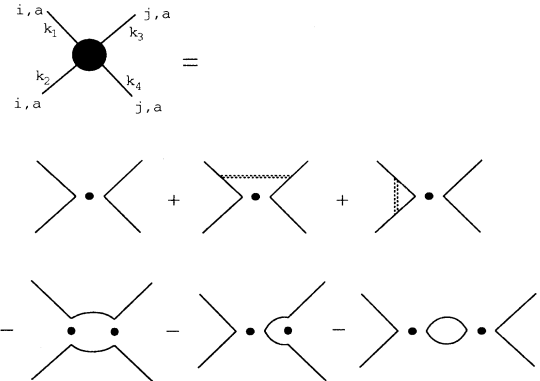


FIG. 12. Diagrams defining the renormalization of μ and λ calculated with the effective Hamiltonian from Eq. (A11) within the replica formalism.

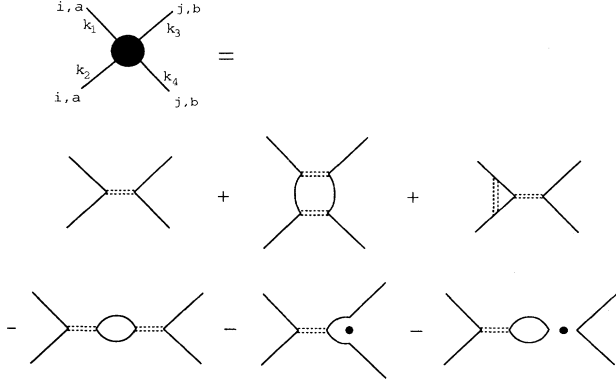


FIG. 13. Diagrams defining the renormalization of $\hat{\sigma}_1$ and $\hat{\sigma}_2$, calculated with the effective Hamiltonian from Eq. (A11), within the replica formalism.

APPENDIX C: ANALYSIS OF THE FLOW NEAR FIXED POINT P_5

In this appendix we calculate the renormalization-group flow near the fixed point P_5 for $D > 4$. For simplicity we will restrict our analysis to an invariant subspace of the full parameter space defined by $\hat{\sigma}_2 = 0$. The generalization to the full space is straightforward.

To calculate the flow near P_5 we need to linearize the set of recursion relations in Eqs. (4.4a)–(4.4c) within the $\hat{\sigma}_2 = 0$ subspace. We can further reduce this three-dimensional problem to the analysis of a two-dimensional parameter subspace defined by $\hat{\mu} + 3\hat{\lambda} = 0$. The reason for this is that this is an attractive and an invariant subspace. To show this we use Eqs. (4.4a) and (4.4b) to construct a recursion relation for $\hat{\mu} + 3\hat{\lambda}$:

$$\begin{aligned} \frac{d(\hat{\mu} + 3\hat{\lambda})}{dl} = & \left[\epsilon - \frac{d_c}{6} (2\hat{\mu} + 3\hat{\lambda}) - \frac{5\hat{\mu}(\hat{\mu} + \hat{\lambda})}{2\hat{\mu} + \hat{\lambda}} + \frac{5}{4}\hat{\sigma}_1 \right. \\ & \left. + \frac{5}{4}\hat{\sigma}_2 \left[\frac{3\hat{\mu}^2}{(2\hat{\mu} + \hat{\lambda})^2} + \frac{2\hat{\lambda}}{2\hat{\mu} + \hat{\lambda}} \right] \right] (\hat{\mu} + 3\hat{\lambda}). \end{aligned} \quad (\text{C1})$$

This reveals that $\hat{\mu} + 3\hat{\lambda} = 0$ is an invariant subspace. To examine the stability of this subspace we expand Eq. (C1) around $\hat{\mu} + 3\hat{\lambda} = 0$ near P_5 in terms of a small deviation $\delta = \hat{\mu} + 3\hat{\lambda}$:

$$\frac{d\delta}{dl} = -\hat{\mu} \frac{d_c + 12}{6} \delta. \quad (\text{C2})$$

Hence $\hat{\mu} + 3\hat{\lambda} = 0$ is an exponentially attractive subspace, provided $\hat{\mu} > 0$.

Inside the two-dimensional subspace the recursion relations Eqs. (4.4) reduce to

$$\frac{d\hat{\mu}}{dl} = -|\epsilon| \hat{\mu} - \frac{d_c + 24}{12} \hat{\mu}^2 + \frac{5}{4} \hat{\mu} \hat{\sigma}_1, \quad (\text{C3a})$$

$$\frac{d\hat{\sigma}_1}{dl} = -|\epsilon| \hat{\sigma}_1 - \frac{d_c + 12}{6} \hat{\sigma}_1 \hat{\mu} + \frac{5}{4} \hat{\sigma}_1^2. \quad (\text{C3b})$$

We linearize the above equations around P_5 defined by $\hat{\mu}^* = 0$ and $\hat{\sigma}_1^* = \frac{4}{5}|\epsilon|$ and obtain

$$\frac{d\hat{\mu}}{dl} = 0, \quad (\text{C4a})$$

$$\frac{d}{dl} \left[\hat{\sigma}_1 - \frac{2(d_c + 12)}{15} \hat{\mu} \right] = |\epsilon| \left[\hat{\sigma}_1 - \frac{2(d_c + 12)}{15} \hat{\mu} \right]. \quad (\text{C4b})$$

The eigenvectors and eigenvalues are easily calculated:

$$\hat{e}_1 = (0, 1), \quad y_1 = |\epsilon|, \quad (\text{C5a})$$

$$\hat{e}_2 = \left[1, \frac{2(d_c + 12)}{15} \right], \quad y_2 = 0. \quad (\text{C5b})$$

As discussed in the main text, the flow is exponentially unstable in the σ_1 direction around P_5 . To study the stability of P_5 in the direction of \hat{e}_2 we rewrite Eq. (C3) with the unstable eigenmode \hat{e}_1 projected out, i.e., along the subspace $\hat{\sigma}_1 - [2(d_c + 12)/15]\hat{\mu} = 0$. We find that the flow is also weakly *unstable* in the temperature direction

$$\frac{d\hat{\mu}}{dl} = \frac{d_c}{12} \hat{\mu}^2. \quad (\text{C6})$$

This equation is easily integrated with the result

$$\hat{\mu}(l) = \frac{\hat{\mu}(l_0)}{1 - (l - l_0) \hat{\mu}(l_0) d_c / 12}, \quad (\text{C7})$$

which leads to the flow illustrated schematically in Fig. 5. The subspace $\hat{\sigma}_1 - [2(d_c + 12)/15]\hat{\mu} = 0$ near P_5 defines the “transition surface” discussed in Sec. IV.

- [1] Y. Kantor, M. Kardar, and D. R. Nelson, *Phys. Rev. A* **35**, 3056 (1987).
 [2] For a review, see the articles in *Statistical Mechanics of Membranes and Interfaces*, edited by D. R. Nelson, T. Piran, and S. Weinberg (World Scientific, Singapore, 1989).
 [3] D. R. Nelson and L. Peliti, *J. Phys. (Paris)* **48**, 1085 (1987).
 [4] Y. Kantor and D. R. Nelson, *Phys. Rev. A* **38**, 4020 (1987).

- [5] F. F. Abraham, W. E. Rudge, and M. Plishke, *Phys. Rev. Lett.* **62**, 1757 (1989); see also M. Plishke and D. Boal, *Phys. Rev. A* **38**, 4943 (1988).
 [6] See, e.g., F. F. Abraham and D. R. Nelson, *Science* **249**, 393 (1990), and *J. Phys. (Paris)* **51**, 2653 (1990). This last reference simulates a “collapsed” self-avoiding membrane with fractal dimension $d_f \approx 3$, as might be expected for a membrane in a solvent. From this point of view, a hypothetical crumpled membrane (with $d_f \approx 2.5$, see Ref. [1])

- would be in an *intermediate* phase, obtainable by varying the solvent quality from good (producing a flat phase) to bad (producing collapse). For an alternative scenario describing the analogue of Θ -point behavior in membranes, see F. Abraham and M. Kardar, *Science* **252**, 419 (1991).
- [7] M. Paczuski, M. Kardar, and D. R. Nelson, *Phys. Rev. Lett.* **60**, 2638 (1988).
- [8] J. A. Aronovitz and T. C. Lubensky, *Phys. Rev. Lett.* **60**, 2634 (1988); J. A. Aronovitz, L. Golubović, and T. C. Lubensky, *J. Phys. (Paris)* **50**, 609 (1989).
- [9] F. David and E. Guitter, *Europhys. Lett.* **5**, 709 (1988); E. Guitter, F. David, S. Leibler, and L. Peliti, *J. Phys. (Paris)* **50**, 1789 (1989).
- [10] A. Blumstein, R. Blumstein, and T. H. Vanderspurt, *J. Colloid Interface Sci.* **31**, 236 (1969).
- [11] A. Elgsaeter, B. Stokke, A. Mikkelsen, and D. Branton, *Science* **234**, 1217 (1986).
- [12] R. Lipowsky and M. Girardet, *Phys. Rev. Lett.* **65**, 2893 (1990).
- [13] S. Leibler (unpublished).
- [14] M. Yamaguchi, M. L. Greaser, and R. G. Cassens, *J. Ultrastructure Res.* **48**, 33 (1974).
- [15] T. Hwa, Ph.D. thesis, MIT, 1990; T. Hwa, E. Kokufuta, and T. Tanaka, *Phys. Rev. A* **44**, 2235 (1991).
- [16] R. R. Chianelli, E. B. Prestridge, T. A. Pecoraro, and J. P. DeNeufville, *Science* **203**, 1105 (1979).
- [17] We exclude here the case of random long-range attractive interactions, which are known to strongly influence the folding of linear protein macromolecules. See, e.g., E. Shaknovich and A. M. Gutin, *J. Phys. A* **22**, 1647 (1989).
- [18] S. P. Obukhov, *J. Phys. A* **19**, 3655 (1986).
- [19] G. S. Grest and M. Murat, *J. Phys. (Paris)* **51**, 1415 (1990).
- [20] D. R. Nelson and L. Radzihovsky, *Europhys. Lett.* (to be published).
- [21] L. Radzihovsky and P. LeDoussal (unpublished).
- [22] We also assume that the polymerized bonds are all approximately equal in length. Bonds of variable length could of course be chosen to relax the frustration caused by the unbound disclinations, and cause the membrane to remain flat when placed in the solvent.
- [23] See, e.g., D. R. Nelson, in *Phase Transitions*, edited by C. Domb and J. Lebowitz (Academic, London 1983), Vol. 7.
- [24] M. Mutz, D. Bensimon, and M. J. Brienne, *Phys. Rev. Lett.* (to be published).
- [25] T. C. Lubensky and J. Prost (unpublished).
- [26] Strictly speaking, our discussion of disclinations applies to liquids initially polymerized in a plane. We expect, however, a similar defect distribution for spherical vesicles, provided the persistence length of the surface normal is large compared to the spacing between unbound disclinations. This appears to be the case for the vesicles studied by Mutz, Bensimon, and Brienne [24].
- [27] We are indebted for discussions with T. C. Lubensky about this kind of randomness.
- [28] Such calculations have recently been carried out by D. Morse and T. C. Lubensky (private communication).
- [29] A. B. Harris, *J. Phys. C* **7**, 1671 (1974).
- [30] Note that $c(\mathbf{x})$ should be identified in general with the local *fluctuation* in impurity concentration, rather than with the impurity concentration itself.
- [31] D. R. Nelson, *Phys. Rev. B* **27**, 2902 (1983).
- [32] For a discussion of how membranes buckle when isolated dislocations or disclinations are present, see S. Seung and D. R. Nelson, *Phys. Rev. A* **38**, 1005 (1988).
- [33] S. Sachdev and D. R. Nelson, *J. Phys. C* **17**, 5473 (1984).
- [34] D. R. Nelson, *Phys. Rev. B* **26**, 269 (1982).
- [35] D. S. Fisher, B. I. Halperin, and R. Morf, *Phys. Rev. B* **19**, 2457 (1979).
- [36] Y. Imry and S. K. Ma, *Phys. Rev. Lett.* **35**, 1399 (1975).
- [37] L. D. Landau and E. M. Lifshitz, *Theory of Elasticity* (Pergamon, New York, 1970).
- [38] R. H. Swendsen and J. S. Wang, *Phys. Rev. Lett.* **57**, 2607 (1986), and references cited therein.
- [39] K. G. Wilson and J. Kogut, *Phys. Rep. C* **12**, 77 (1974).
- [40] S. F. Edwards and P. W. Anderson, *J. Phys. F* **5**, 965 (1975).